DASA 1336

# TECHNICAL PROGRESS REPORT



**DEFENSE ATOMIC SUPPORT AGENCY**

**WASHINGTON 25, D.C.**

DASA-1336

# TRANSLATIONAL EFFECTS OF AIR BLAST FROM HIGH EXPLOSIVES

I. Gerald Bowen
Paul B. Woodworth
Mary E. Franklin
Clayton S. White, M. D.

Presented before
The Symposium on Effectiveness Analysis
Techniques for Non-Nuclear Warheads Against
Surface Targets, U. S. Naval Weapons Laboratory
Dahlgren, Virginia, October 30, 1962

This work, an aspect of investigations dealing with the Biological Effects of Blast from Bombs, was supported by the Defense Atomic Support Agency of the Department of Defense and is being submitted as a Technical Progress Report on Contract No. DA-49-146-XZ-055.



Lovelace Foundation for Medical Education and Research
Albuquerque, New Mexico
November 7, 1962

# CHAPTER 1 INTRODUCTION AND SUMMARY

A portion of the studies of the biological effects of blast from nuclear explosions has been concerned with the translational effects of blast waves for objects as small as a 10-mg stone and as large as a 168-lb man. Computed results from theoretical studies[1,2] when compared to field data for near-ideal blast waves from nuclear explosions[3,4,5] have demonstrated that the motion of experimental objects can be satisfactorily predicted for free-field conditions or for window glass in houses.

This report presents for high explosives (free-air burst) the results of a similar theoretical study – specifically, computed velocity, displacement, and acceleration as functions of time for a variety of objects exposed to blast waves with 12 maximum overpressures ranging from 1 to 20 atm. Although all computations were made for 1 ton of high explosives burst in free air, the results may be readily scaled to lower or higher yields and to surface bursts. The translated objects, or missiles, are identified in this study by their acceleration coefficients* which range from 0.01 to 6.0 $ft^2/lb$.**

---

*Acceleration coefficient is defined for an object as its area presented to the wind times its drag coefficient divided by its mass. See Ref. 2.

**This range in acceleration coefficients is for 1 ton of high explosives burst in free air. Because of scaling laws (see Sect. 2.1), different ranges would apply to other yields and to surface bursts.

REFERENCES CHAPTER 1


1. Bowen, I. G., R. W. Albright, E. R. Fletcher and C. S. White, A Model Designed to Predict the Motion of Objects Translated by Classical Blast Waves, Civil Effects Test Operations, USAEC Report CEX-58.9, June 29, 1961.

2. Fletcher, E. R., R. W. Albright, V. C. Goldizen and I. G. Bowen, Determinations of Aerodynamic-Drag Parameters of Small Irregular Objects by Means of Drop Tests, Civil Effects Test Operations, USAEC Report CEX-59.14, October 1961.

3. Bowen, I. G., A. F. Strehler and M. B. Wetherbe, Distribution and Density of Missiles from Nuclear Explosions, Operation Teapot Report, WT-1168, December 1956.

4. Bowen, I. G., Mary E. Franklin, E. R. Fletcher and R. W. Albright, Secondary Missiles Generated by Nuclear-Produced Blast Waves, Operation Plumbbob Project 33.2 Report WT-1468, submitted to Mr. L. Joe Deal, Division of Biology and Medicine, U. S. Atomic Energy Commission, on March 7, 1962. (in press)

5. Taborelli, R. V., I. G. Bowen and E. R. Fletcher, Tertiary Effects of Blast—Displacement, Operation Plumbbob Report, WT-1469, May 22, 1959.

## CHAPTER 2 ANALYTICAL PROCEDURES

### 2.1 THE MODEL

The computational model used in this work was reported in Ref. 1 and will not be described in detail. In the previous study tabular values of computed velocity, displacement, and acceleration as functions of time were presented as nondimensional quantitites for missiles produced by nuclear blast waves. However, to make interpretation of the results easier, the computations in the present study for missiles produced by high-explosive blast waves were made in dimensional form for a yield of 1 ton,* and the results are presented graphically. Dimensional analysis derived previously[1] make it possible to apply the results to explosions of lower or higher yields within the limits of weapons' scaling.

In deriving the computational model (see Ref. 1), the following assumptions were made: (1) Friction between the missile (translated object) and the surface was negligible. (2) The effect of gravity on the horizontal velocity of the missile could be neglected. (3) Only the winds associated with the blast wave contributed to missile translation. (4) The acceleration coefficient of the missile could be assumed to be constant. (5) The blast wave does not decay appreciably while passing the missile.

Allowance was made for the object being exposed to the blast winds for a time dependent on the relative velocity of the missile and the blast wave. This effect was particularly important for the missiles with the higher acceleration coefficients which are propelled to relatively high velocities.

Numerical solutions of the model were determined by stepwise integration of the model equations.[1] For missile velocity, the following was used

$$\Delta v = e + f - \sqrt{e^2 + f^2 + 2 f g} \qquad (1)$$

where

$\Delta v$ is positive if $\underline{u} > v_1$,

$\Delta v$ is negative if $\underline{u} > v_1$,

$\Delta v$ = change in missile velocity during time step $\Delta t$,

$e = \dot{\underline{x}} - v_1$,

*For free-air bursts.

$f = \alpha \underline{q} (\underline{u} - v_i) \dot{\underline{x}} \Delta t / \underline{u}^2$,

$g = \dot{\underline{x}} - \underline{u}$,

and

$v_i$ = missile velocity at beginning of $\Delta t$,

$\underline{u}$ = average wind velocity during $\Delta t$,

$\underline{x}$ = average velocity of propagation of blast wave during $\Delta t$, approximated by $\dot{\underline{x}} = 0.6\, \underline{u} + \sqrt{c_o^2 + .36\, \underline{u}^2}$

$c_o$ = velocity of sound in the undisturbed air

$\alpha$ = acceleration coefficient = $s\, C_d / m$,

$s$ = area presented to wind by missile,

$C_d$ = drag coefficient of missile,

$m$ = mass of missile, and

$\underline{q}$ = average dynamic pressure during $\Delta t$.

Incremental distance, $\Delta d$, was computed by the following:

$$\Delta d = (v_o + \Delta v/2)\, \Delta t\, \dot{\underline{x}} / (\dot{\underline{x}} - v_o - \Delta v/2) \qquad (2)$$

Missile acceleration, a, was determined from the following (integration being unnecessary):

$$a = \frac{dv}{dt} = q\, \alpha\, (u - v)^2 / u^2 \qquad (3)$$

where q, u, and v are dynamic pressure, wind velocity, and missile velocity at any time t. (Note that an acceleration numeric is used in Chap. 3: $A = a/g$ where g is the acceleration of gravity.)

Equations (1) and (2) were integrated in a stepwise fashion from the arrival time of the blast wave ($t = 0$) to the time of zero wind velocity ($t = t_u^+$). Because of rapid changes in missile and wind velocities shortly after the arrival of the blast wave, it was necessary to use smaller time steps during the early times than during later times. The following arbitrary scheme was used to determine the variable time step. The first step was always $0.001\, t_u^+$. The remaining time ($t_u^+ - 0.001\, t_u^+$) was divided into 99 log intervals. The first 85 of the log intervals were used as ever-increasing time

steps. The 85th log interval was then used as a constant time step until time $t_u^+$ was reached.

For convenience, the scaling laws for translational studies derived in Chaps. 2 and 5 of Ref. 1 will be restated using the terminology of the present report. The subscript "1" is used to denote parameters applicable to a yield of 1 ton of high explosives,* to an ambient speed of sound of 1117 ft/sec, and to an ambient pressure of 14.7 psi. The parameters without subscripts are applicable to a yield of W tons, to an ambient speed of sound of $c_o$ ft/sec, and to an ambient pressure of $p_o$ psi. Thus, the results in Chap. 3 can be scaled as follows for free-air bursts (for surface bursts, replace W by 2W):

$$v = v_1 (c_o/1117),$$

$$d = d_1 (14.7\ W/p_o)^{1/3},$$

$$A = A_1 (c_o/1117)^2 (1/W)^{1/3} (p_o/14.7)^{1/3},$$

$$t = t_1 (1117/c_o) (14.7\ W/p_o)^{1/3}, \text{ and}$$

$$a = a_1 (14.7/p_o)^{2/3} (c_o/1117)^2 (1/W)^{1/3}$$

where

$v$ = missile velocity in ft/sec,

$c_o$ = ambient speed of sound in ft/sec,

$d$ = distance of missile travel in ft,

$W$ = yield of high explosives* in tons (for surface bursts, replace W by 2W),

$p_o$ = ambient pressure in psi,

$A$ = acceleration of missile ($A = a/32.2$) in gravity units,

$t$ = time after arrival of blast wave in msec, and

$a$ = acceleration coefficient ($a = s\ C_d/m$) in $ft^2/lb$.

## 2.2 BLAST-WAVE PARAMETERS

### 2.2.1 General

The solution of the translation model described in the last section requires that dynamic pressure (q) and wind velocity (u) be

---

*For free-air bursts.

defined as a function of time. Clear and explicit presentations of these quantities for high explosives were not found in the literature. Consequently, most of the blast material used in this report was taken from a numerical study by Brode[2] and from experimental results reported by Goodman.[3] This material, along with Rankine-Hugoniot equations,[4] allowed computation of the needed blast parameters. The overpressure-time relation, needed to determine wind velocity as a function of time, will be treated first.

2.2.2 Overpressure vs. Time

The overpressure information was obtained from experimental results.[3] Duration and overpressure impulse scaled to 1 ton of high explosives are recorded in Table 2.1 for the overpressure values of interest in this study. Overpressure as a function of time was not defined in Ref. 3, but in the present report it was assumed to be of the form

$$P = P_s (1 - T)e^{-nT} \tag{4}$$

where

$P$ = overpressure in atm,

$P_s$ = maximum or shock overpressure in atm,

$T = t/t_p^+$,

$t$ = time after arrival of the blast wave in msec,

$t_p^+$ = duration of positive overpressure in msec, and

$n$ = a constant for a given value of $P_s$.

Since n in the above equation determines the shape of the P-t curve, it also determines the impulse, $\int_0^{t_p^+} P\,dt$, for particular values of $P_s$ and $t_p^+$. Thus, integrating Eq. (4) gives the following impulse, $I_p^+$, relation:

$$I_p^+ = P_s t_p^+ (e^{-n} + n - 1)/n^2 \tag{5}$$

The values of n listed in Table 2.1 were found using Eq. (5).

Table 2.1

Parameters for Determining Overpressure-time Functions*
(1 Ton of High Explosives, Free-Air Burst)

| $P_s$, atm | $t_p^+$, msec | $I_p^+$, atm msec | n |
|---|---|---|---|
| 1.0 | 16.5 | 6.48 | .960 |
| 1.5 | 14.4 | 7.55 | 1.32 |
| 2.0 | 12.9 | 8.30 | 1.47 |
| 2.5 | 11.7 | 8.91 | 1.65 |
| 3.0 | 10.9 | 9.46 | 1.81 |
| 4.0 | 9.70 | 10.3 | 2.15 |
| 5.0 | 8.87 | 10.9 | 2.42 |
| 6.0 | 8.40 | 11.4 | 2.80 |
| 8.0 | 7.99 | 12.2 | 3.63 |
| 10.0 | 7.73 | 12.7 | 4.40 |
| 15.0 | 6.27 | 13.6 | 5.19 |
| 20.0 | 3.00 | 14.2 | 2.65 |

*$P = P_s (1 - T) e^{-nT}$ where $T = t/t_p^+$

## 2.2.3 Dynamic Pressure vs. Time

Dynamic pressure in atmospheres at the shock front, $Q_s$, was computed using the Rankine-Hugoniot relation reported in Ref. 4:

$$Q_s = \frac{2.5\ P_s^2}{7 + P_s}. \tag{6}$$

Values of $Q_s$ corresponding to $P_s$ values used in this study are listed in the second column of Table 2.2. Durations, $t_q^+$, and impulses, $I_q^+$, for dynamic pressure in the same table were obtained by scaling the results of a numerical study[2] to a yield of 1 ton (free-air burst). A scaling factor was applied to the numerical results in order to make the overpressure durations consistent with those found experimentally.[3]

A procedure similar to that described in Sect. 2.2.2 was used to determine dynamic pressure vs. time. Values recorded in Table 2.4 for r were obtained from

$$I_q^+ = Q_s\, t_q^+ (e^{-r} + r - 1)/r^2 \tag{7}$$

where

$Q_s$ = maximum or shock dynamic pressure in atm,

$t_q^+$ = duration of positive dynamic pressure in msec, and

r = a constant for a particular value of $P_s$ or $Q_s$.

Dynamic pressure as a function of time could then be found using

$$Q = Q_s (1 - T)\, e^{-rT}$$

where $T = t/t_q^+$.

## 2.2.4 Wind Velocity vs. Time

By definition,

$$q = 1/2\ \rho u^2 \tag{8}$$

where q = dynamic pressure,

Table 2.2

Parameters for Determining Dynamic Pressure as a Function of Time*
(1 Ton of High Explosives, Free-Air Burst)

| $P_s$, atm | $Q_s$, atm** | $t_u^+$, msec | $I_u^+$, atm msec | r |
|---|---|---|---|---|
| 1.0 | .3125 | 23.4 | 1.56 | 3.33 |
| 1.5 | .6618 | 20.4 | 2.14 | 5.10 |
| 2.0 | 1.111 | 18.4 | 2.72 | 6.31 |
| 2.5 | 1.645 | 17.1 | 3.26 | 7.47 |
| 3.0 | 2.250 | 16.1 | 3.80 | 8.39 |
| 4.0 | 3.635 | 14.4 | 4.80 | 9.80 |
| 5.0 | 5.208 | 13.1 | 5.77 | 10.7 |
| 6.0 | 6.923 | 11.9 | 6.65 | 11.3 |
| 8.0 | 10.667 | 9.85 | 8.68 | 11.0 |
| 10.0 | 14.706 | 8.17 | 10.81 | 10.9 |
| 15.0 | 25.568 | 5.06 | 16.43 | 8.69 |
| 20.0 | 35.556 | 3.00 | 22.19 | 5.46 |

*$Q = Q_s (1 - T) e^{-rT}$ where $T = t/t_u^+$

**Computed from $Q_s = \frac{2.5 P_s^2}{7 + P_s}$

$\rho$ = air density, and

u = wind velocity.

Wind velocity could thus be determined after the dynamic pressure and the air density were evaluated. The air density across the shock, $\rho_s$, was found using one of the Rankine-Hugoniot equations:[4]

$$\rho_s = \rho_0 (7 + 6 P_s)/(7 + P_s) \qquad (9)$$

where $\rho_0$ is the ambient air density.

Changes in air density after the passage of the shock were assumed to be adiabatic. Thus,

$$\rho = \rho_s \left(\frac{P + 1}{P_s + 1}\right)^{1/1.4} \qquad (10)$$

where $\rho$ = air density when the overpressure is P atm.

## REFERENCES CHAPTER 2


1. Bowen, I. G., R. W. Albright, E. R. Fletcher and C. S. White, A Model Designed to Predict the Motion of Objects Translated by Classical Blast Waves, Civil Effects Test Operations, USAEC Report CEX-58.9, June 29, 1961.

2. Brode, Harold L., A Calculation of the Blast Wave From a Spherical Charge of TNT, RM-1965, ASTIA Document Number AD 144302, August 21, 1957.

3. Goodman, H. J., Compiled Free-Air Blast Data on Bare Spherical Pentolite, BRL Report No. 1092, February 1960.

4. Glasstone, Samuel, Editor, The Effects of Nuclear Weapons, Revised Edition 1962, Superintendent of Documents, U. S. Printing Office, Washington, D. C., April 1962.

## CHAPTER 3 RESULTS

### 3.1 GENERAL

Computed results were obtained using the translation model described in Sect. 2.1 and a digital computer with an incremental plotter to graph the output data. The system for determining time steps (see Sect. 2.1) resulted in 106 to 112 steps for each numerical integration from the arrival of the blast wave ($t = 0$) to the time of zero wind ($t = t_u^+$).

As previously noted, all solutions were made for 1 ton of high explosives for free-air bursts. The 12 different blast waves used are identified in terms of overpressure: $P_s = p_s/p_o$, the ratio of shock overpressure to local ambient pressure (not necessarily the sea-level value of 14.7 psi), sometimes called excess pressure ratio. Values of $P_s$ used were 1.0, 1.5, 2.0, 2.5, 3.0, 4.0, 5.0, 6.0, 8.0, 10.0, 15.0, and 20.0 atm.

For each $P_s$, numerical integrations were made for the following acceleration coefficients, $a_1$, in the order listed: 6, 3, 2, 1, 0.6, 0.3, 0.2, 0.1, 0.06, 0.03, 0.02, 0.01 $ft^2/lb$. If the maximum velocity computed for any acceleration coefficient was less than 10 ft/sec, the computations were halted for that overpressure.

According to the translational model used, the behavior of an object is determined by its acceleration coefficient, all other factors being constant. To aid interpretation of the computed results, a list of acceleration coefficients obtained from Ref. 1 for a variety of objects is reproduced in Table 3.1. A more complete source of acceleration-coefficient information can be found in Ref. 2.

### 3.2 VELOCITY VS. TIME AND DISTANCE VS. TIME

Computed velocity and distance as functions of time are presented for a maximum overpressure* of 1 atm in Figs. 3.1 and 3.2, respectively, for seven acceleration coefficients. Machine plots for these and succeeding figures connected with straight lines every other computed point for the first 86 time steps. All of the remaining time steps were plotted. Each of the curves end at the midpoint of the last time step before the dynamic pressure

*Defined in Sect. 3.1.

Table 3.1

Typical Acceleration Coefficients,* $a = sC_d/m$
where s is the area presented to wind by missile,
$C_d$ is the drag coefficient of the missile,
and m is the mass of the missile

| | $a$, $ft^2/lb$ |
|---|---|
| 168-lb man* | |
| Standing facing wind | 0.052 |
| Standing sidewise to wind | 0.022 |
| Crouching facing wind | 0.021 |
| Crouching sidewise to wind | 0.017 |
| Prone aligned with wind | 0.0063 |
| Prone perpendicular to wind | 0.022 |
| Average value for tumbling man in straight, rigid position | 0.03 |
| 21-g mice, maximum area presented to wind | 0.38 |
| 180-g rats, maximum area presented to wind | 0.19 |
| 530-g guinea pigs, maximum area presented to wind | 0.15 |
| 2100-g rabbits, maximum area presented to wind | 0.079 |
| Typical stones* | |
| 0.1 g | 0.67 |
| 1.0 g | 0.32 |
| 10.0 g | 0.15 |
| Window-glass fragments, 1/8 in. thick** | |
| 0.1 g, all orientations | 0.78 |
| 1.0 g, edgewise and broadside to wind | 0.48-0.57 |
| 10.0 g, edgewise and broadside to wind | 0.34-0.72 |

*From Ref. 1.
**Single-strength window glass. See Ref. 2 for data on plate glass.

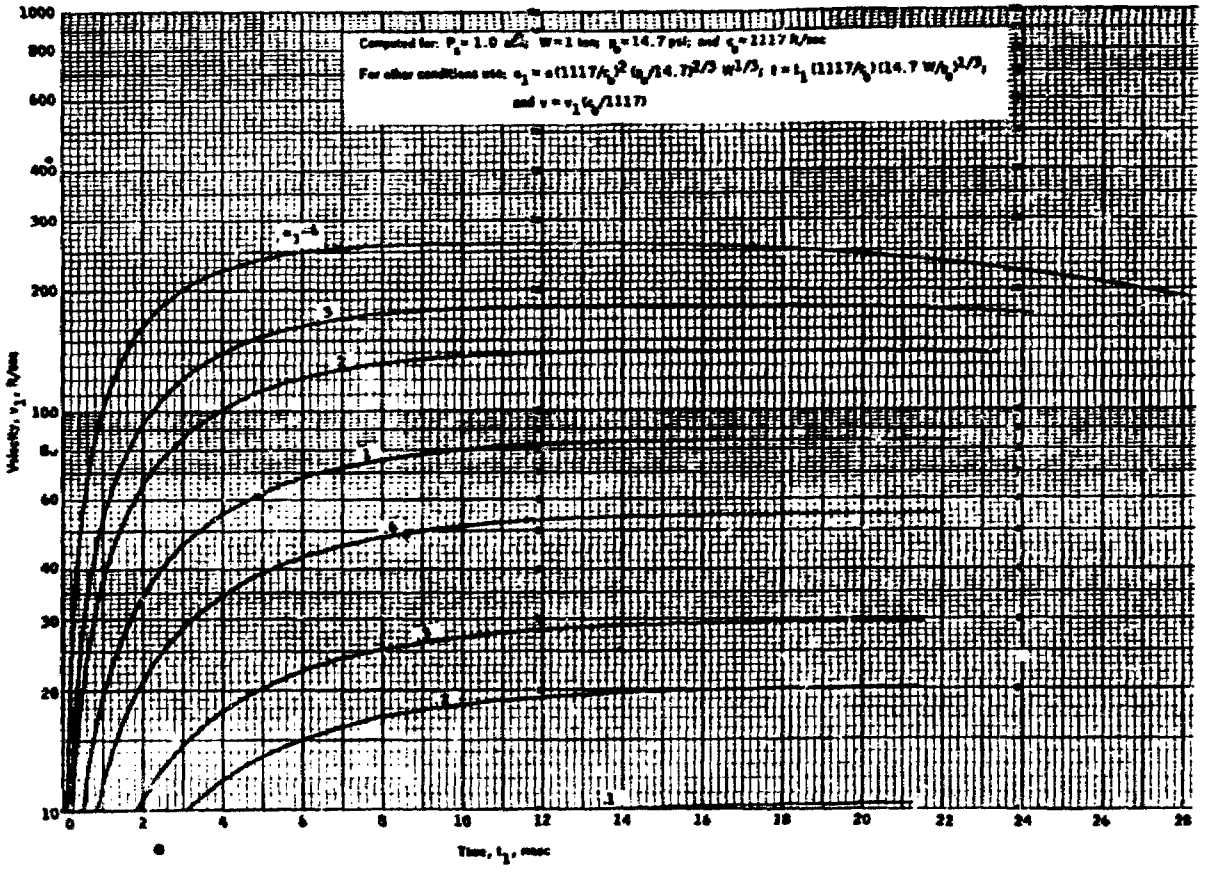


F.g. 3.1 Velocity vs. Time for $P_s$ = 1.0 atm

$W_o$ = 1 ton for free-air burst or 0.5 ton for surface burst.

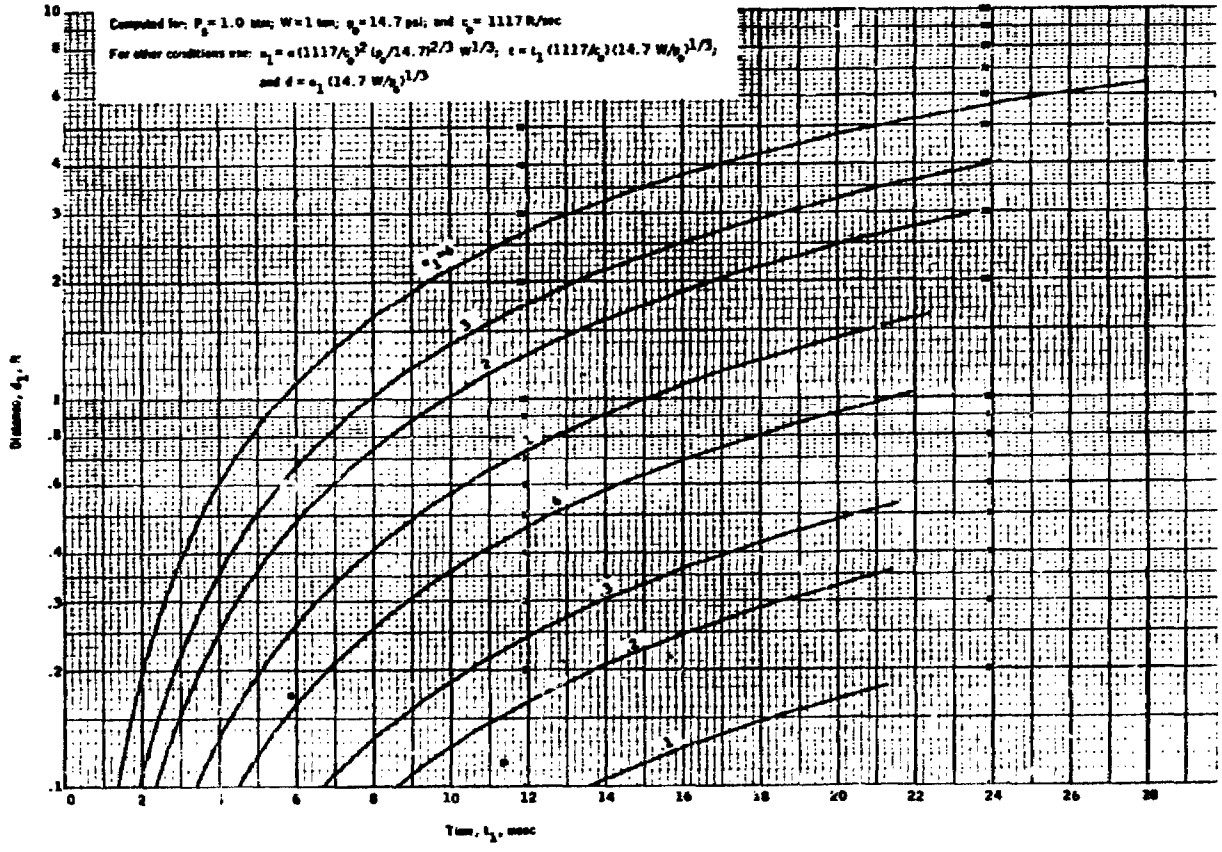


Fig. 3.2 Distance vs. Time for $P_s$ = 1.0 atm

W = 1 ton for free-air burst or 0.5 ton for surface burst.

and winds become negative. For high acceleration coefficients, the curves terminate at later times than do those for low ones: the missiles with high coefficients — and, thus, with high velocities — travel along with the blast wave for longer times than do those with the low ones.

The appropriate equations for scaling the computed results to other yields and ambient pressures and speeds of sound are presented on each chart. To illustrate scaling from 1 ton to 1000 tons (1 kt) and to compare the results for 1 kt with those for nuclear blast waves,[1] consider the maximum velocity and distance of travel at maximum velocity predicted for a 1-g stone when $P_s = 1.0$ atm, $p_o = 14.7$ psi, $c_o = 1117$ ft/sec. A stone of 1 g has an acceleration coefficient of 0.32 $ft^2/lb$. (See Table 3.1.) For a yield of 1 ton* the maximum predicted velocity for $a_1 = 0.32$ $ft^2/lb$ obtained from Fig. 3.1 is about 30 ft/sec occurring 19 msec after the arrival of the blast wave. By referring to Fig. 3.2, the distance of travel of 19 msec is found to be about 0.48 ft.

To apply the computed data to a yield of 1000 tons surface burst, it is first necessary to determine an equivalent acceleration coefficient, $a_1$, for a yield of 0.5 ton surface burst. By using the scaling equation for acceleration coefficient in Figs. 3.1 and 3.2, $a_1 = 0.32$ $ft^2/lb \times (2000)^{1/3} = 4.03$ $ft^2/lb$. The maximum velocity predicted for this value of $a_1$ is about 210 ft/sec occurring 12 msec after the arrival of the blast wave (Fig. 3.1). The distance traveled for W = 0.5 ton and for $a_1 = 4.03$ $ft^2/lb$ at 12 msec is 2.1 ft (Fig. 3.2). For W = 1000 tons, the distance is 2.1 ft $\times (2000)^{1/3} = 26$ ft occurring 12 msec $\times (2000)^{1/3} = 151$ msec after the arrival of the blast wave. For comparison, the maximum velocity and distance of travel at maximum velocity computed for a nuclear blast wave[1] for the conditions stated above for a yield of 1 kt are 200 ft/sec (high explosives: 210 ft/sec) and 28.7 ft (high explosives: 26 ft). A similar comparison was made for an acceleration coefficient of 0.0238 $ft^2/lb$ and a blast wave with a maximum overpressure of 1 atm. The high-explosive data scaled to 1 kt predicts a maximum velocity of 29 ft/sec and the nuclear data a velocity of 30 ft/sec.

The charts shown in Figs. 3.3 to 3.24, similar to those described, were computed for maximum overpressures of 1.5, 2.0, 2.5, 3.0,

---

*The data in the charts were computed for 1 ton for the free-air blast waves or 0.5-ton surface burst.

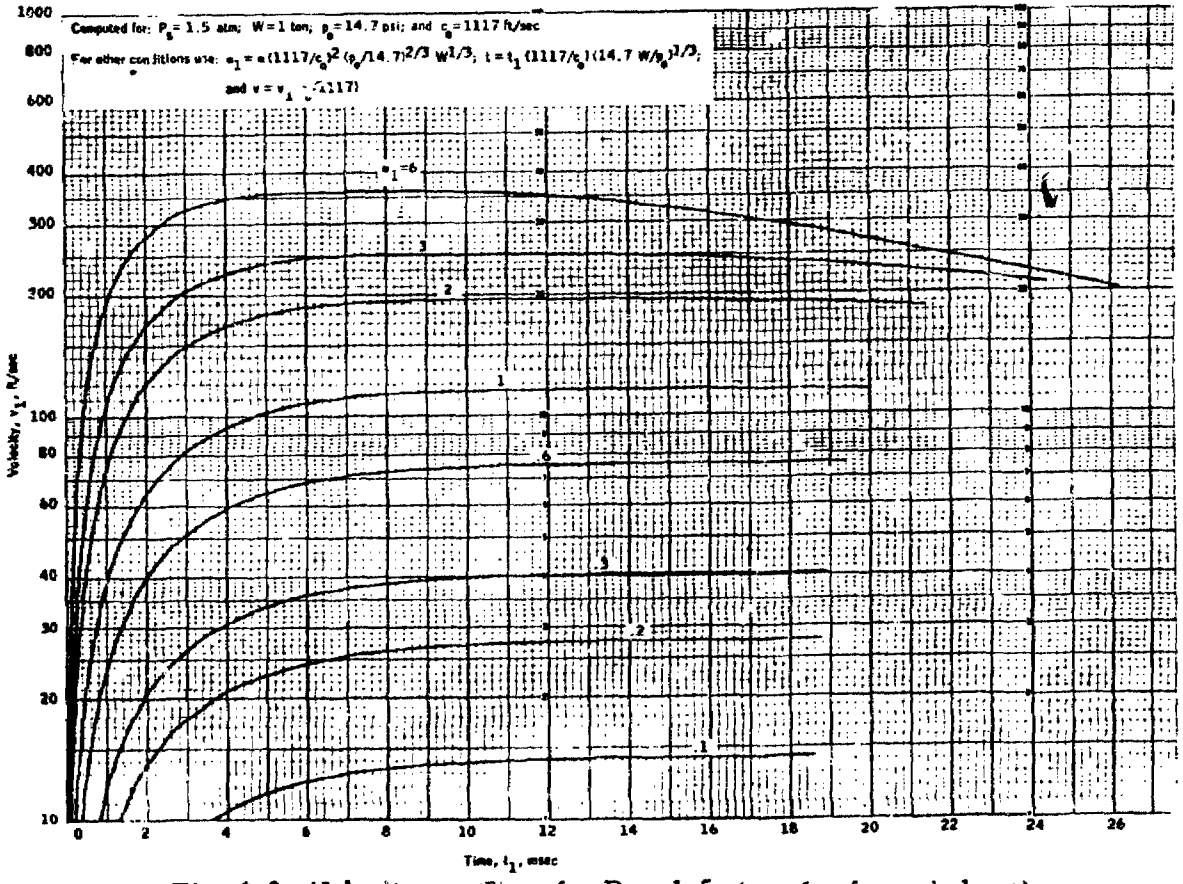


Fig. 3.3 Velocity vs. Time for $P_s$ = 1.5 atm for free-air bursts

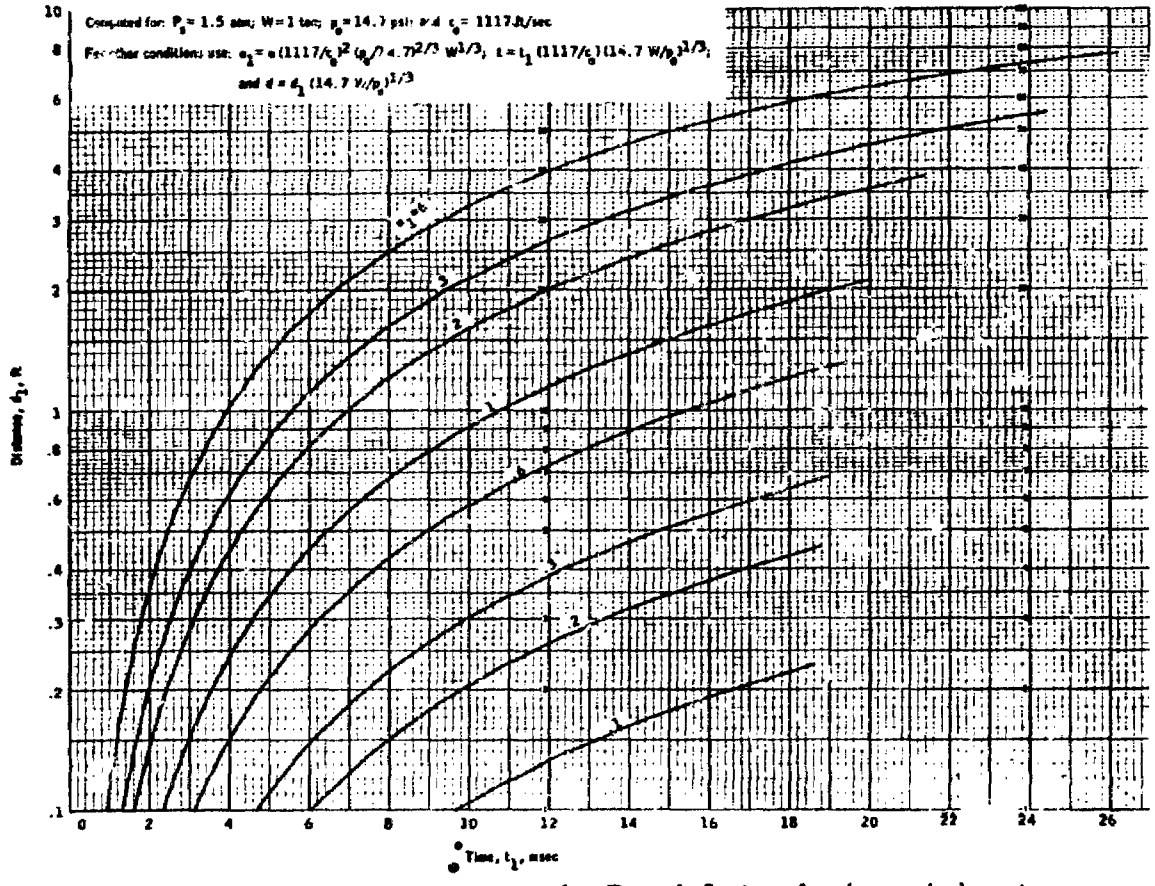


Fig. 3.4 Distance vs. Time for $P_s$ = 1.5 atm for free-air bursts

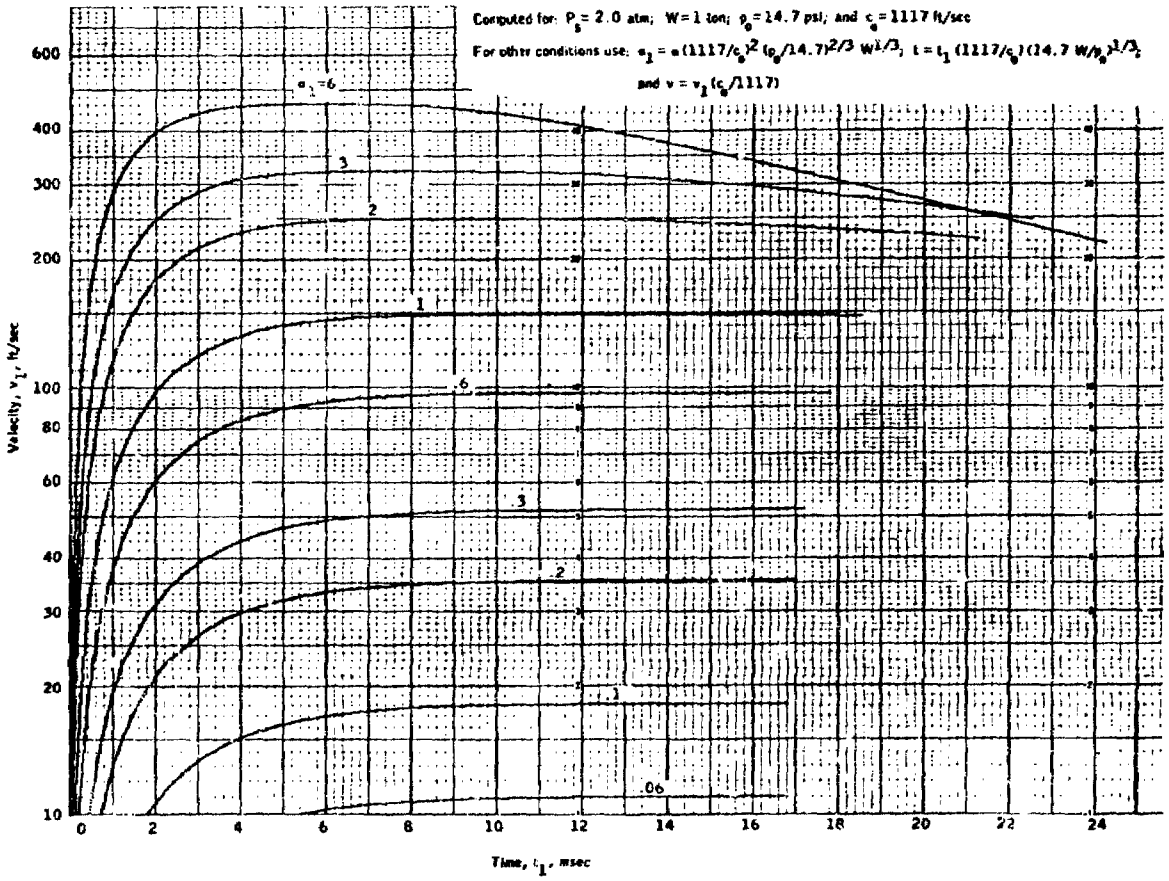


Fig. 3.5 Velocity vs. Time for $P_s$ = 2.0 atm for free-air bursts

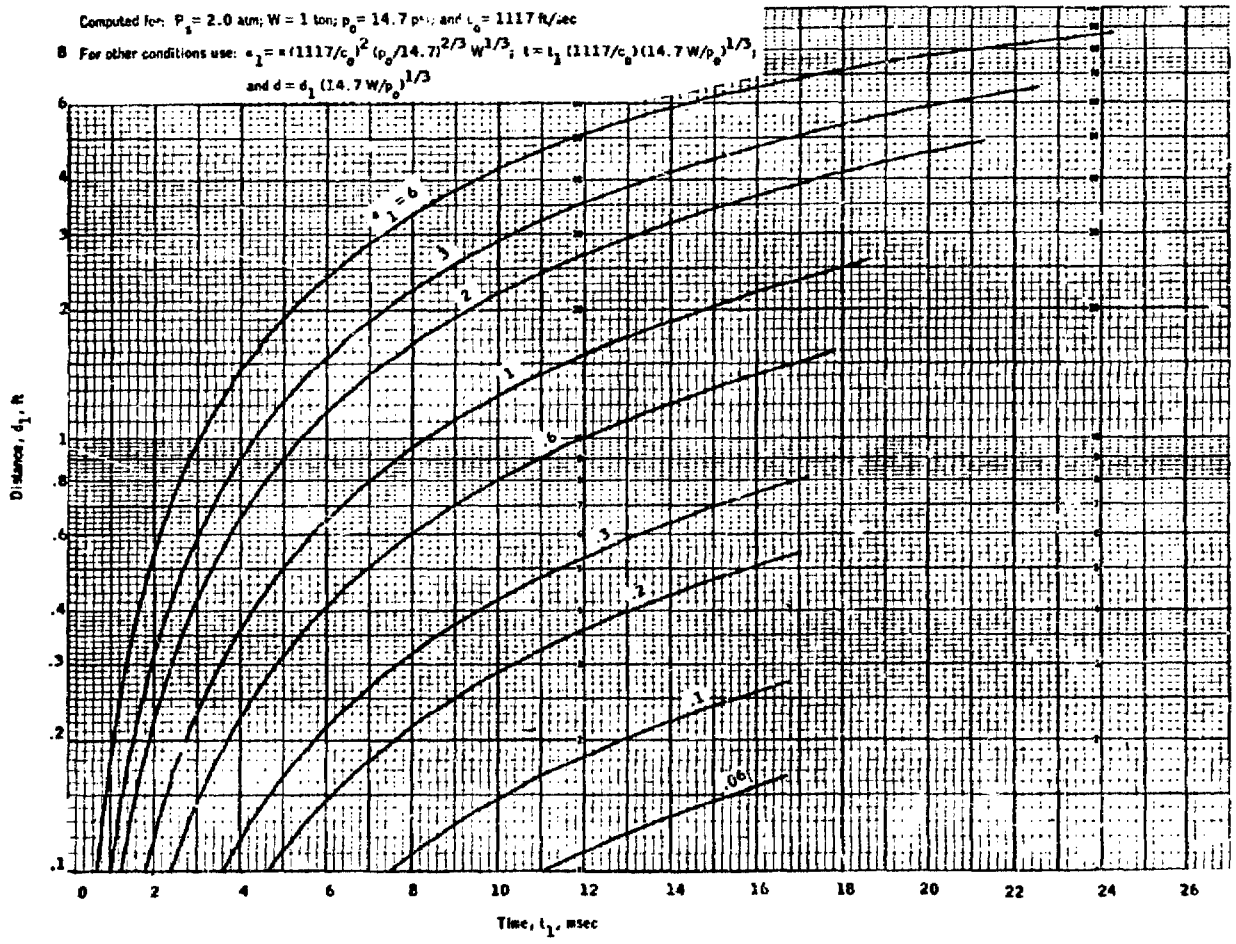


Fig. 3.6 Distance vs. Time for $P_s$ = 2.0 atm for free-air bursts

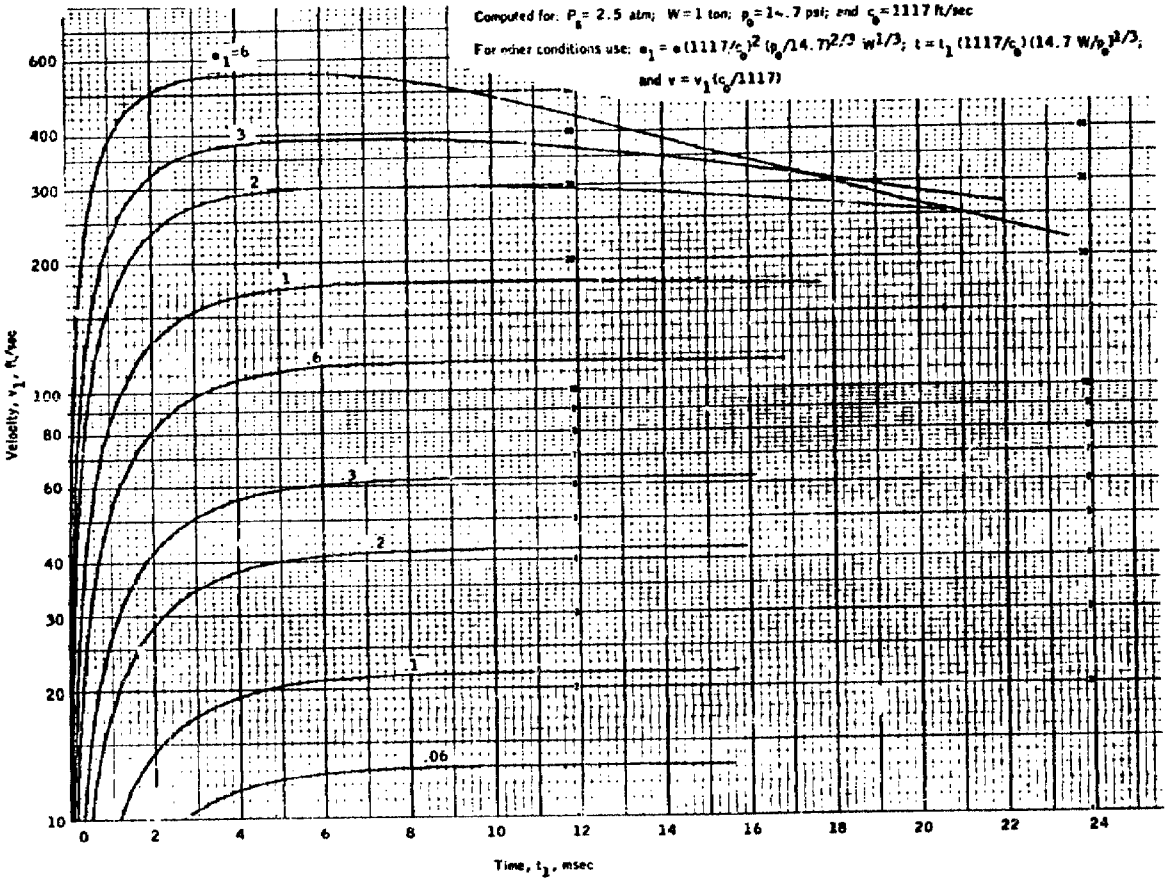


Fig. 3.7 Velocity vs. Time for $P_s$ = 2.5 atm for free-air bursts

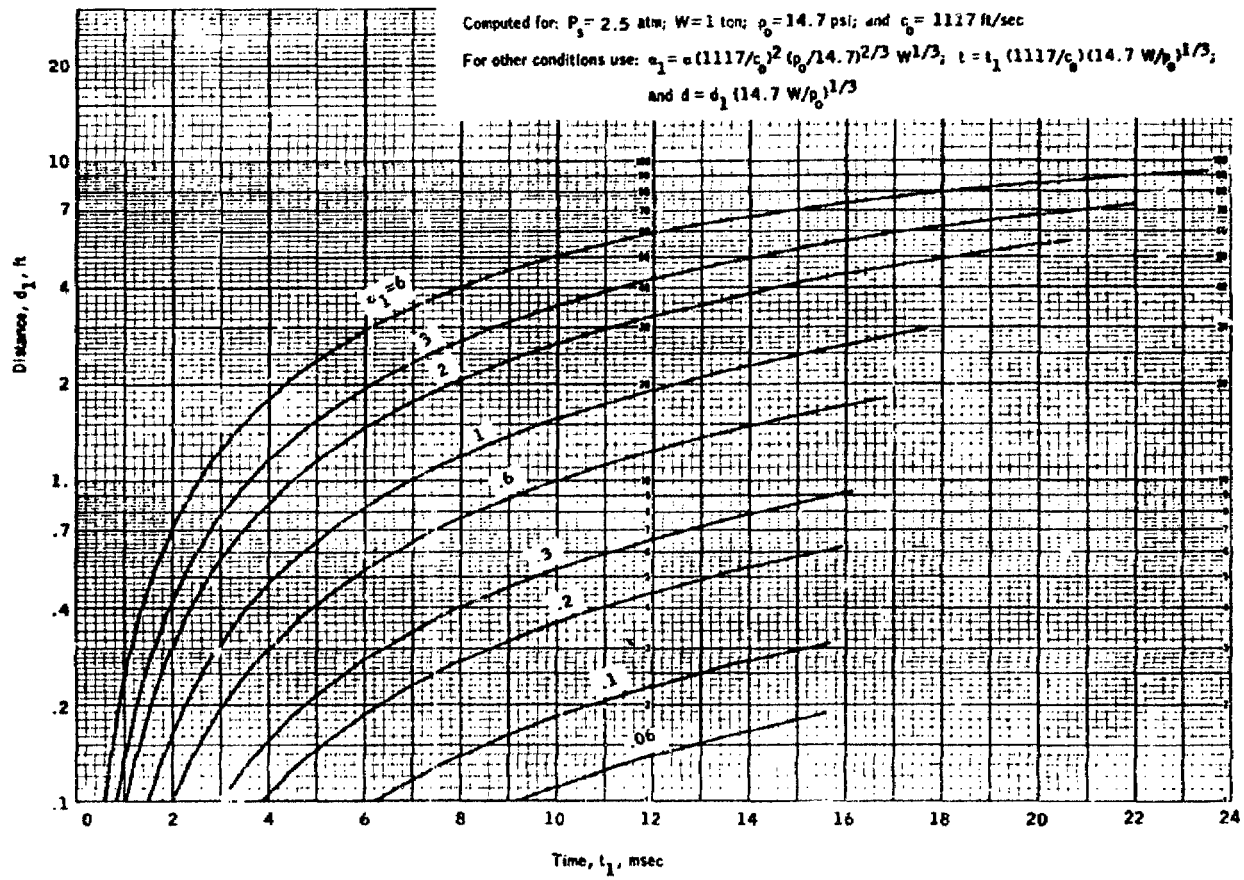


Fig. 3.8 Distance vs. Time for $P_s$ = 2.5 atm for free-air bursts

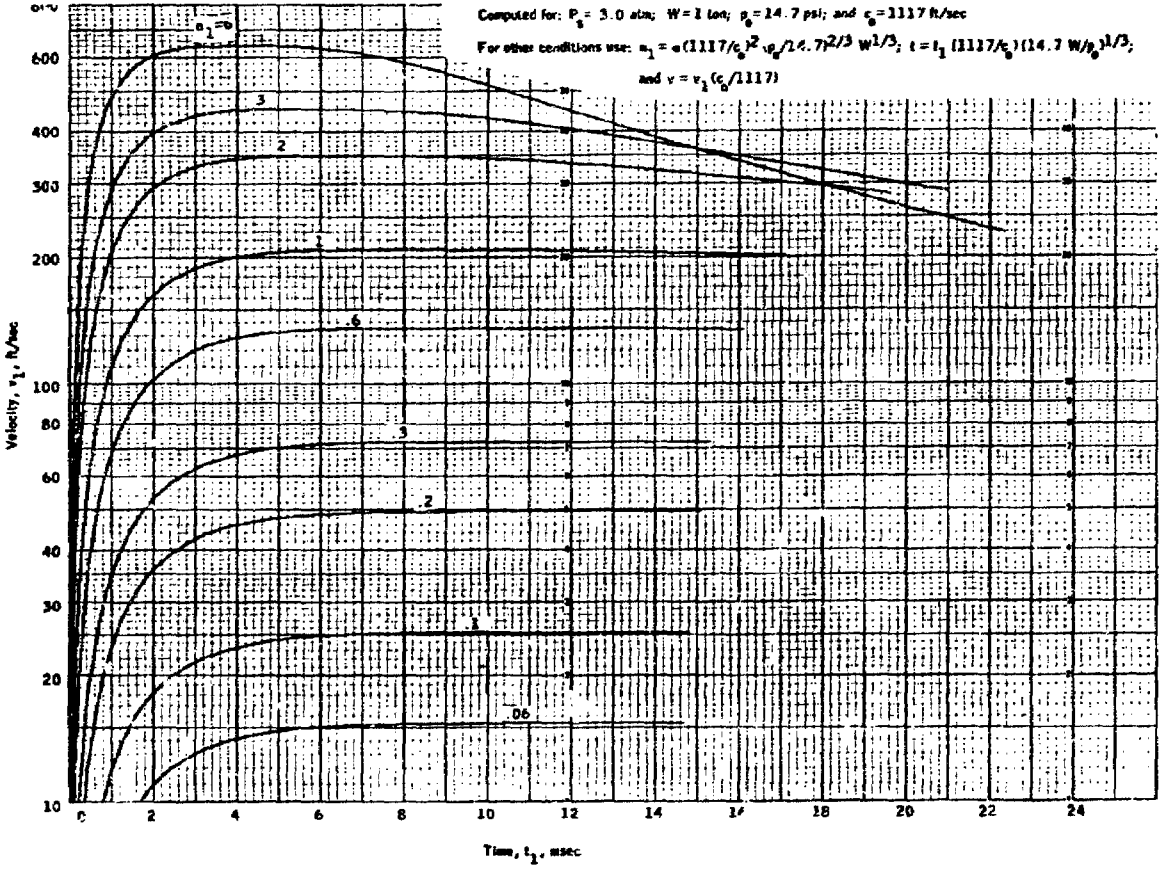


Fig. 3.9 Velocity vs. Time for $P_s$ = 3.0 atm for free-air bursts

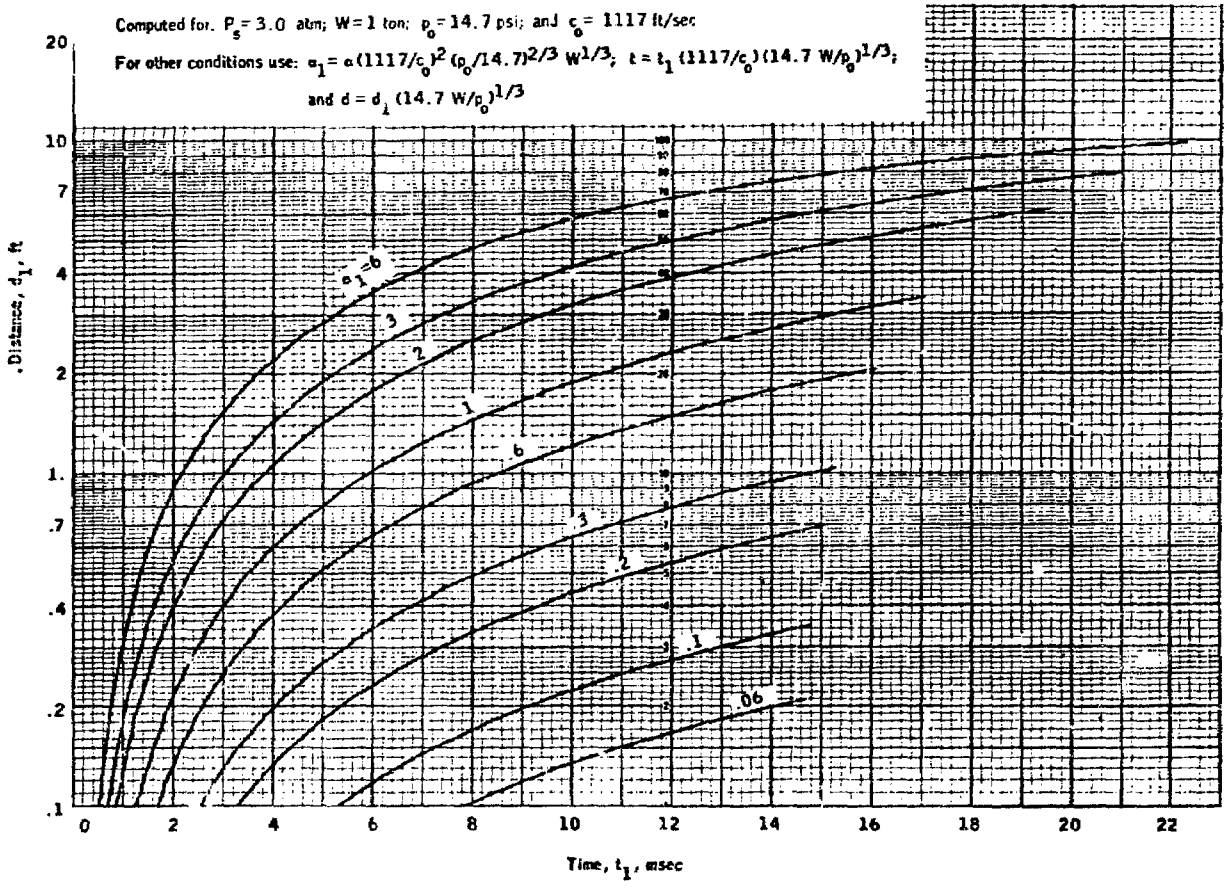


Fig. 3.10 Distance vs. Time for $P_s$ = 3.0 atm for free-air bursts

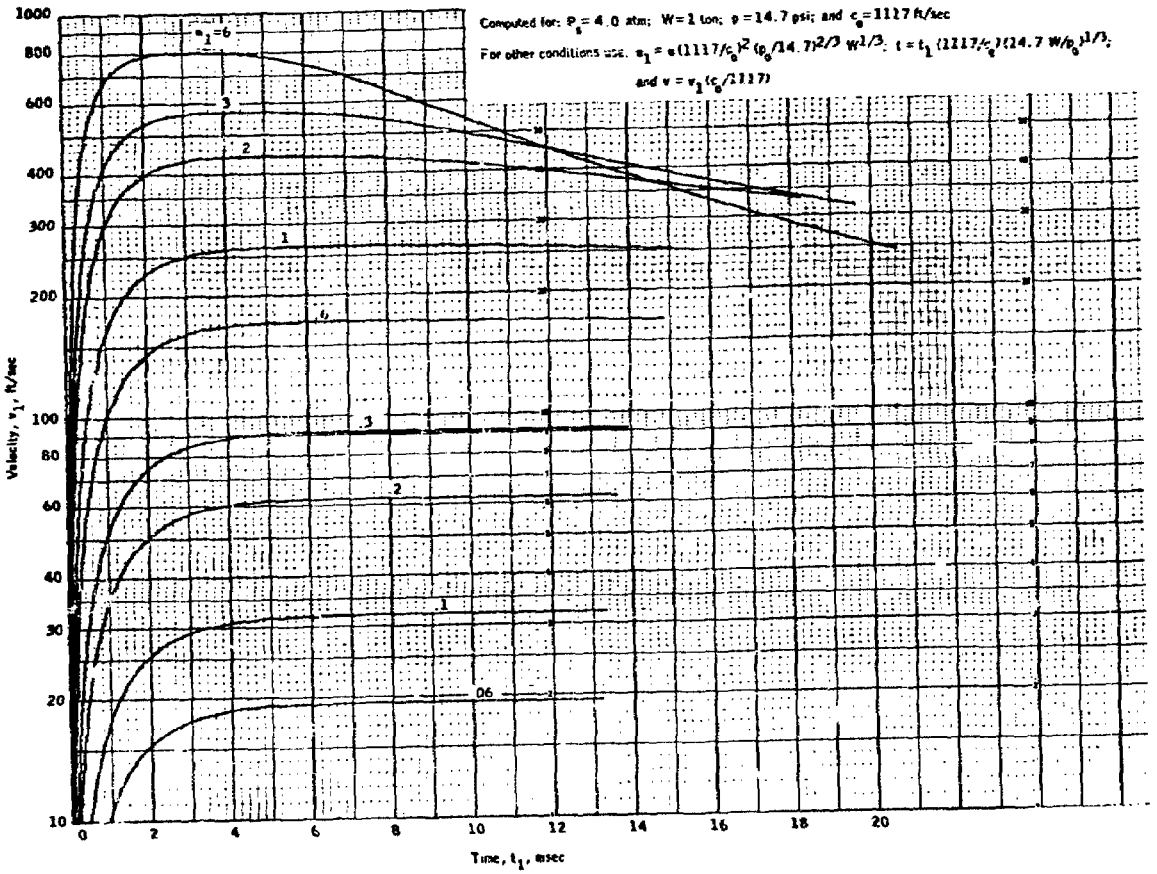


Fig. 3.11 Velocity vs. Time for $P_s$ = 4.0 atm for free-air bursts

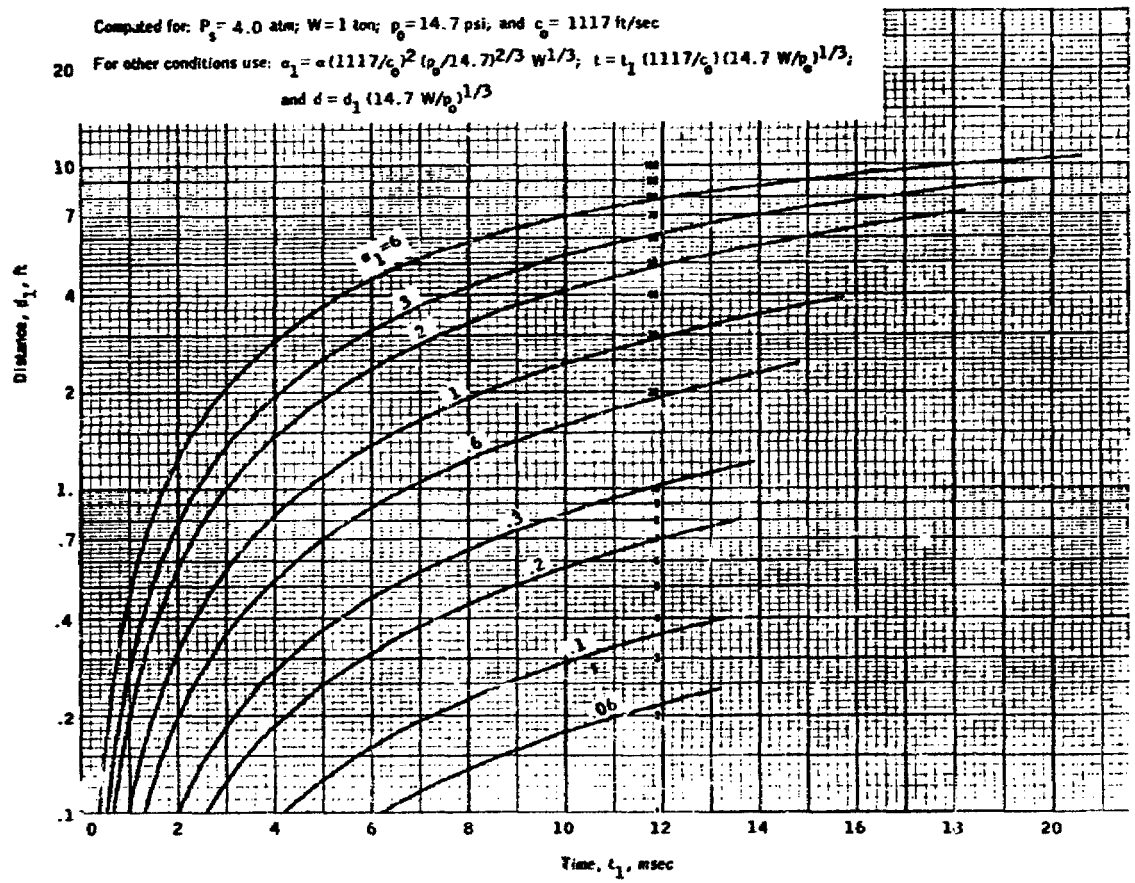


Fig. 3.12 Distance vs. Time for $P_s$ = 4.0 atm for free-air bursts

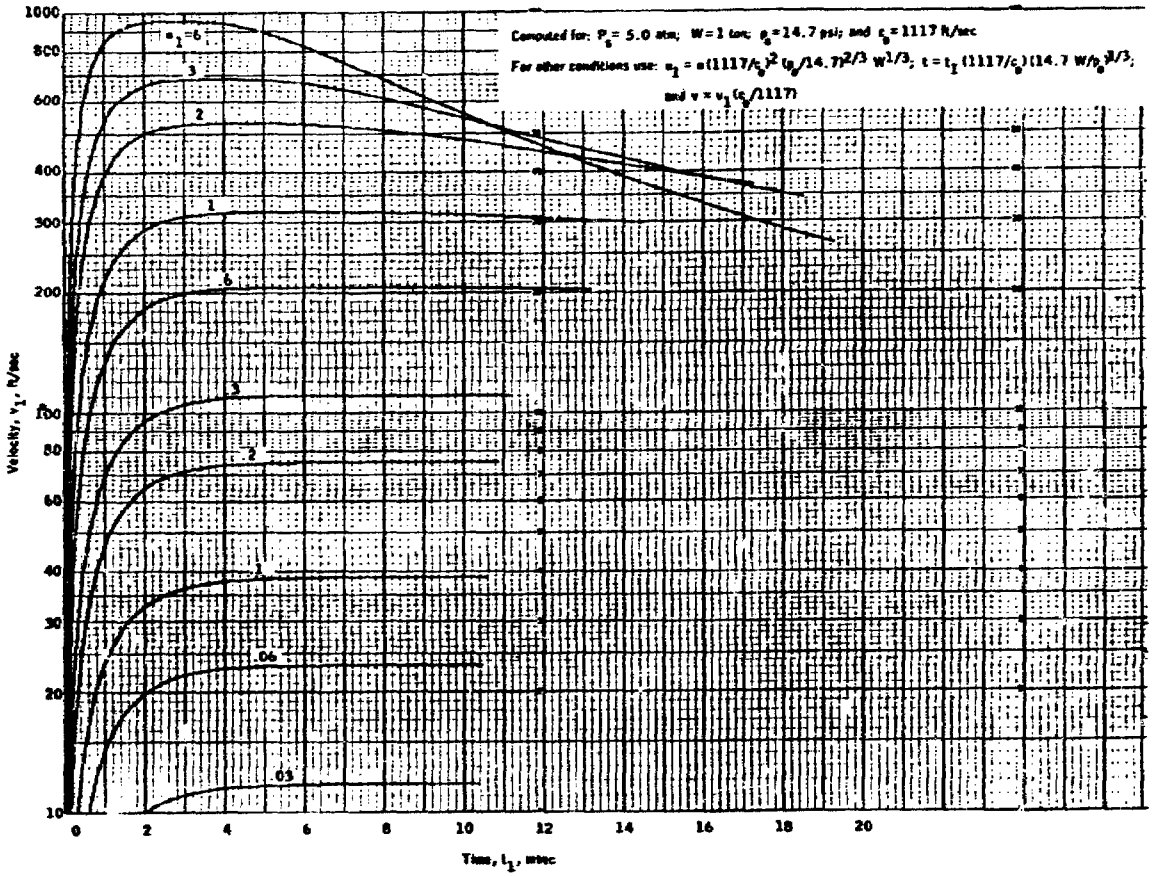


Fig. 3.13 Velocity vs. Time for $P_s$ = 5.0 atm for free-air bursts

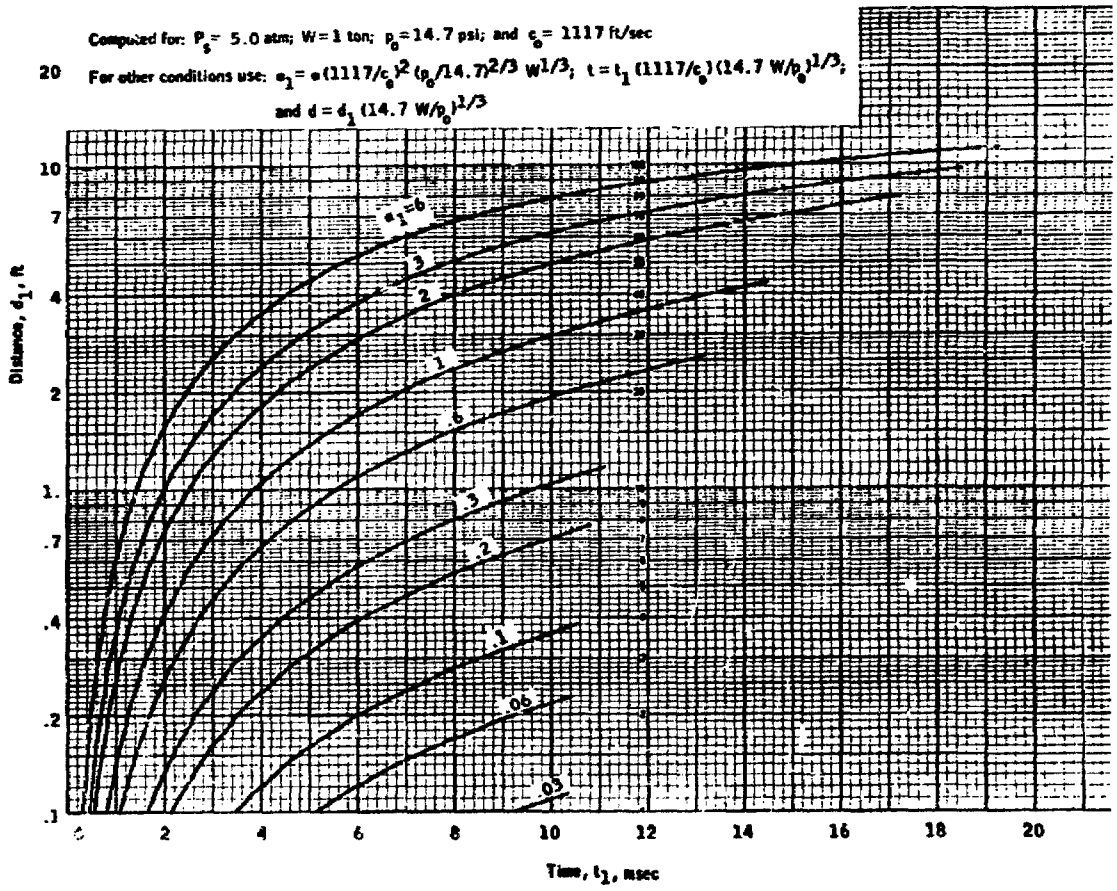


Fig. 3.14 Distance vs. Time for $P_s$ = 5.0 atm for free-air bursts

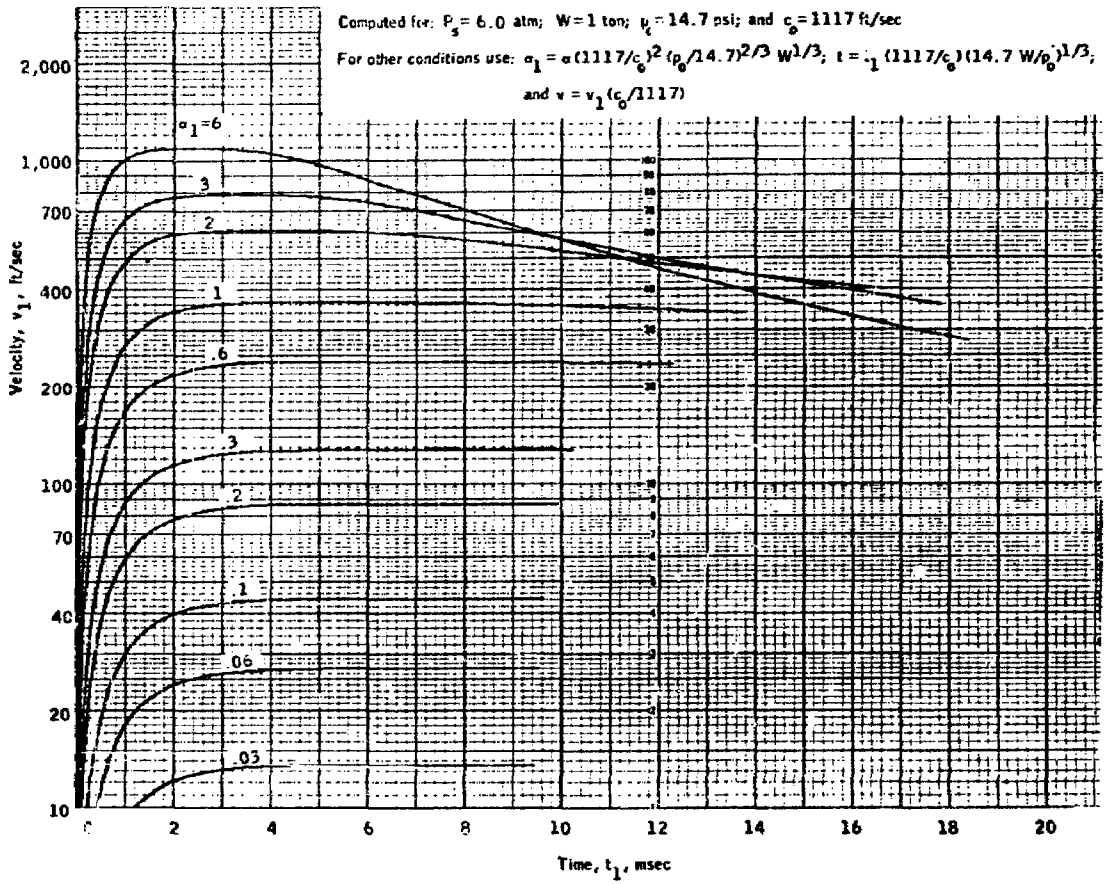


Fig. 3.15 Velocity vs. Time for $P_s$ = 6.0 atm for free-air bursts

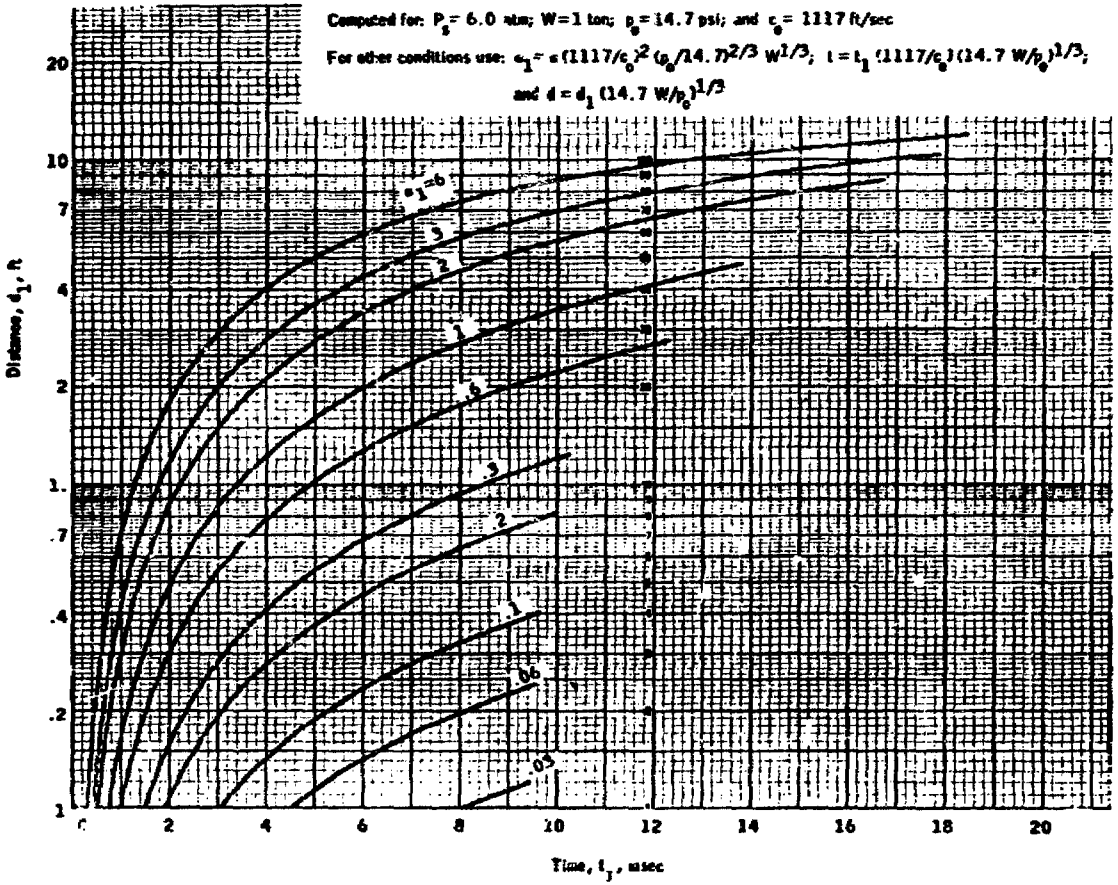


Fig. 3.16 Distance vs. Time for $P_s$ = 6.0 atm for free-air bursts

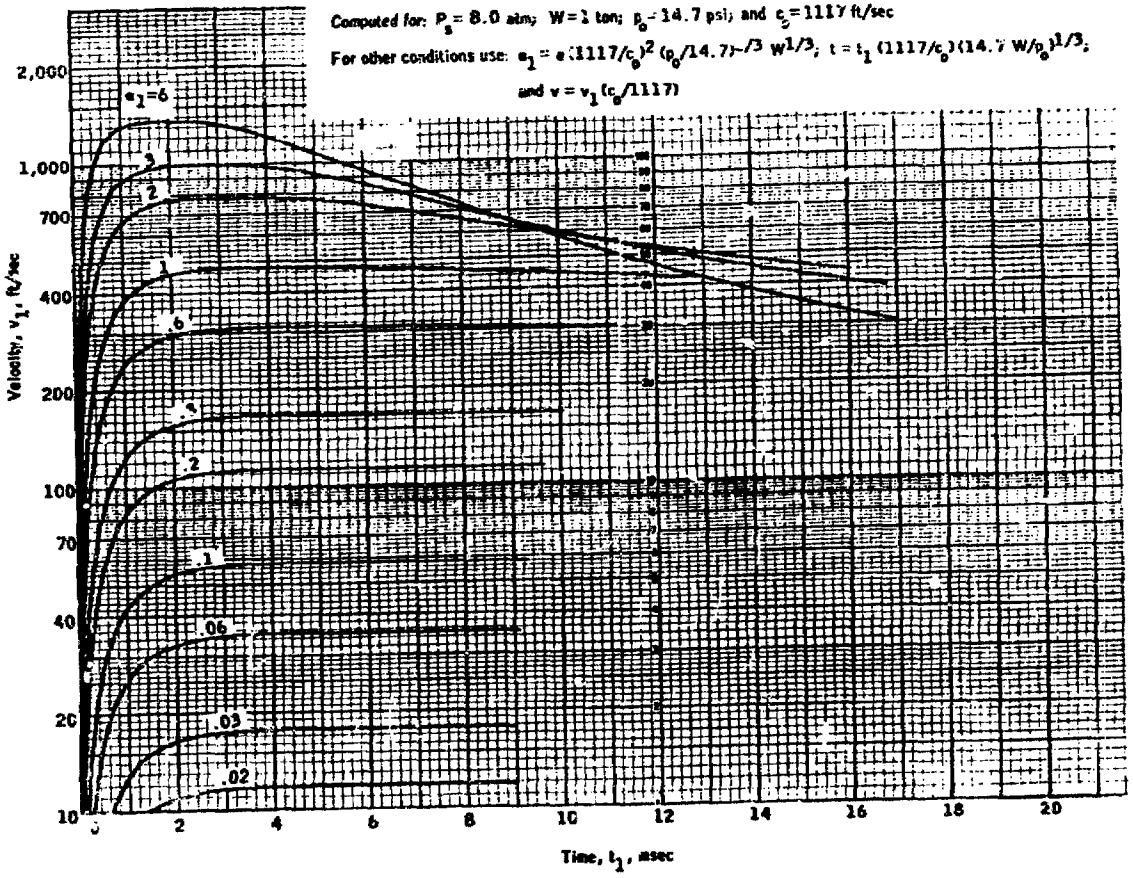


Fig. 3.17 Velocity vs. Time for $P_s$ = 8.0 atm for free-air bursts

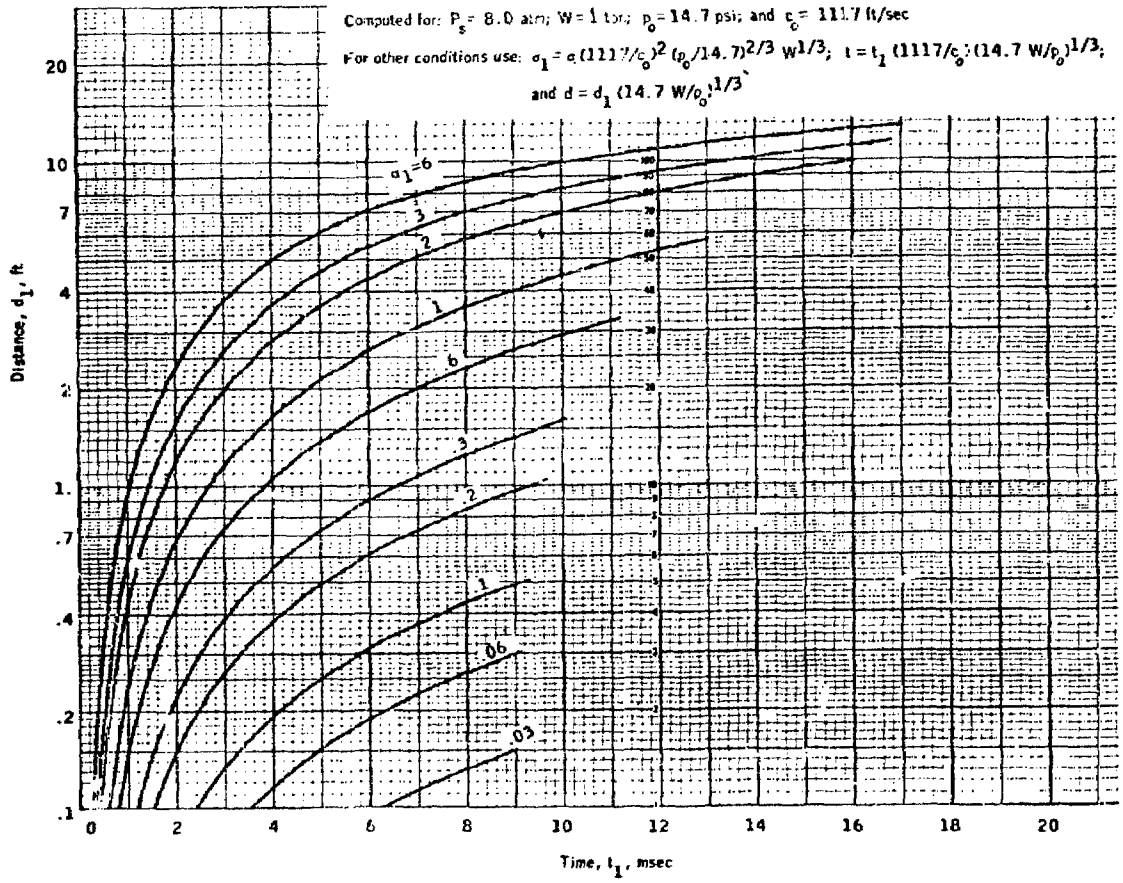


Fig. 3.18 Distance vs. Time for $P_s$ = 8.0 atm for free-air bursts

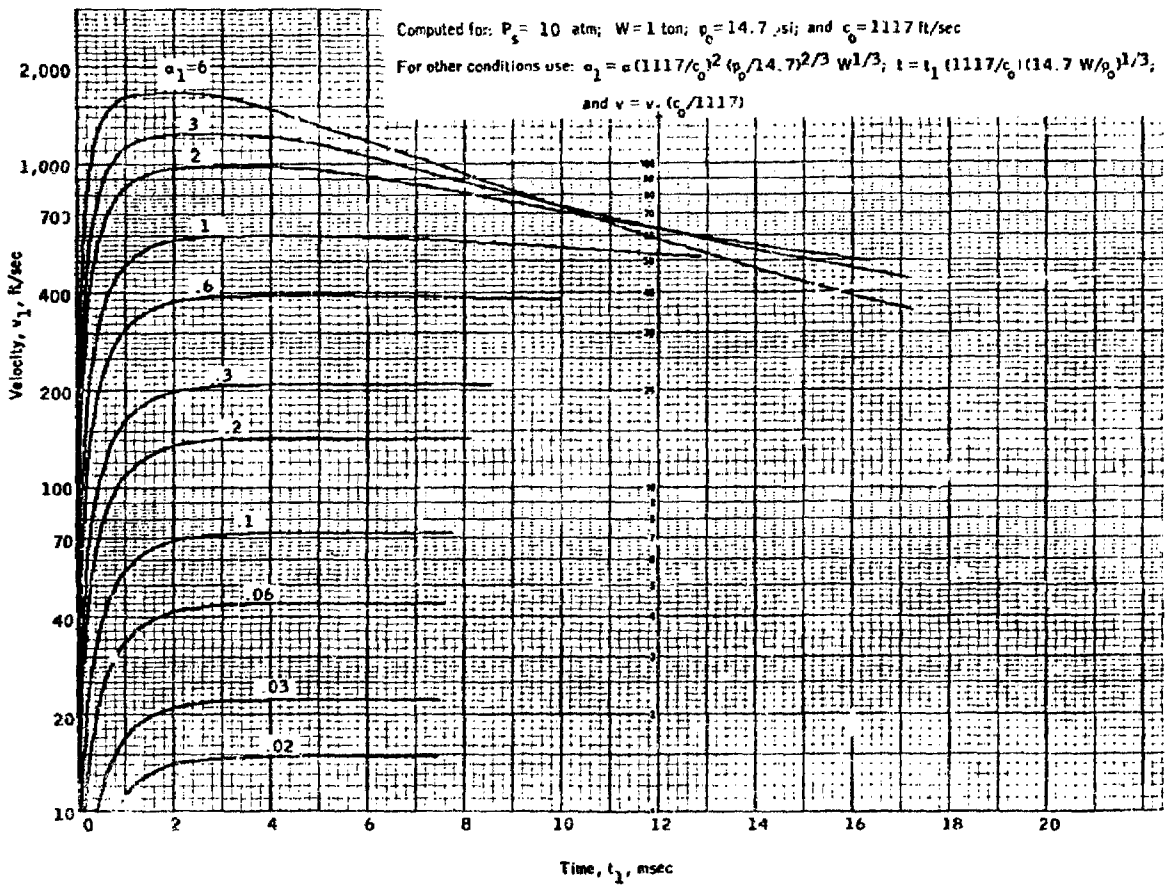


Fig. 3.19 Velocity vs. Time for $P_s$ = 10.0 atm for free-air bursts

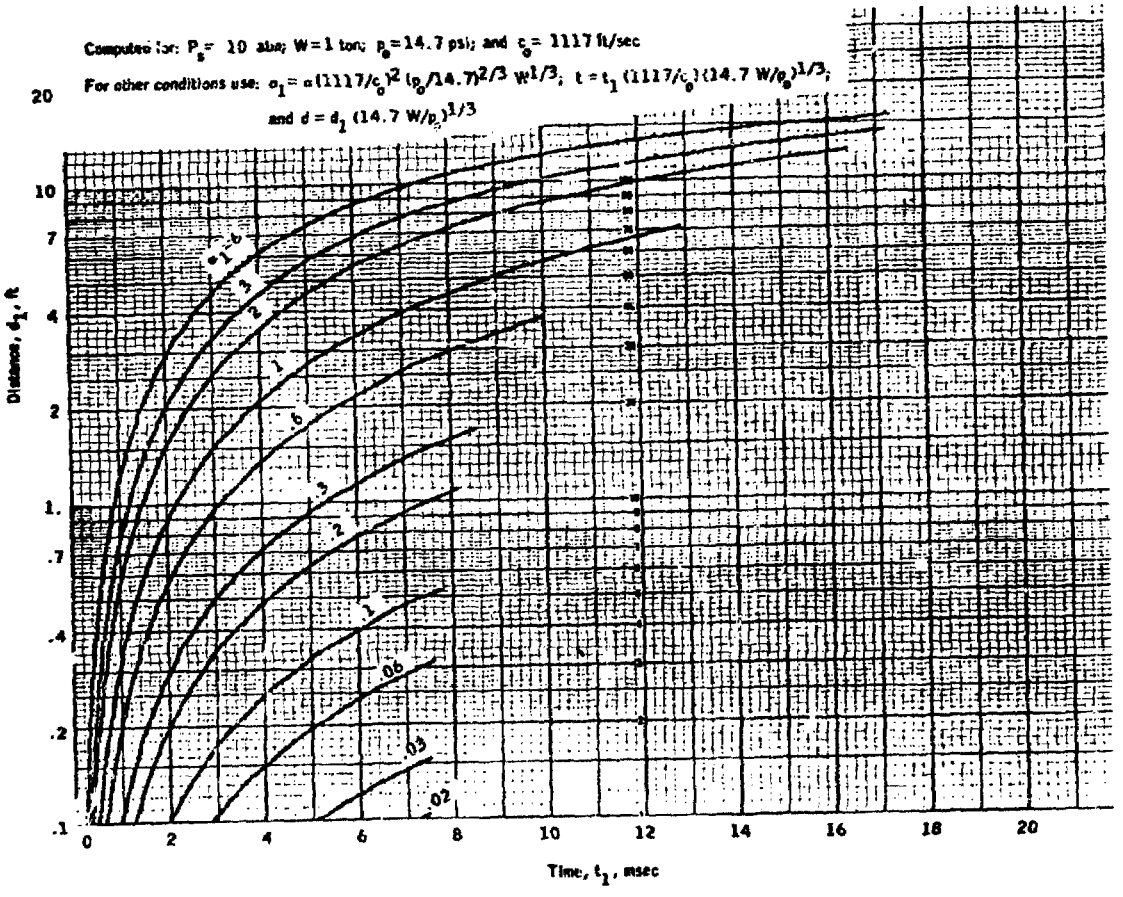


Fig. 3.20 Distance vs. Time for $P_s$ = 10.0 atm for free-air bursts

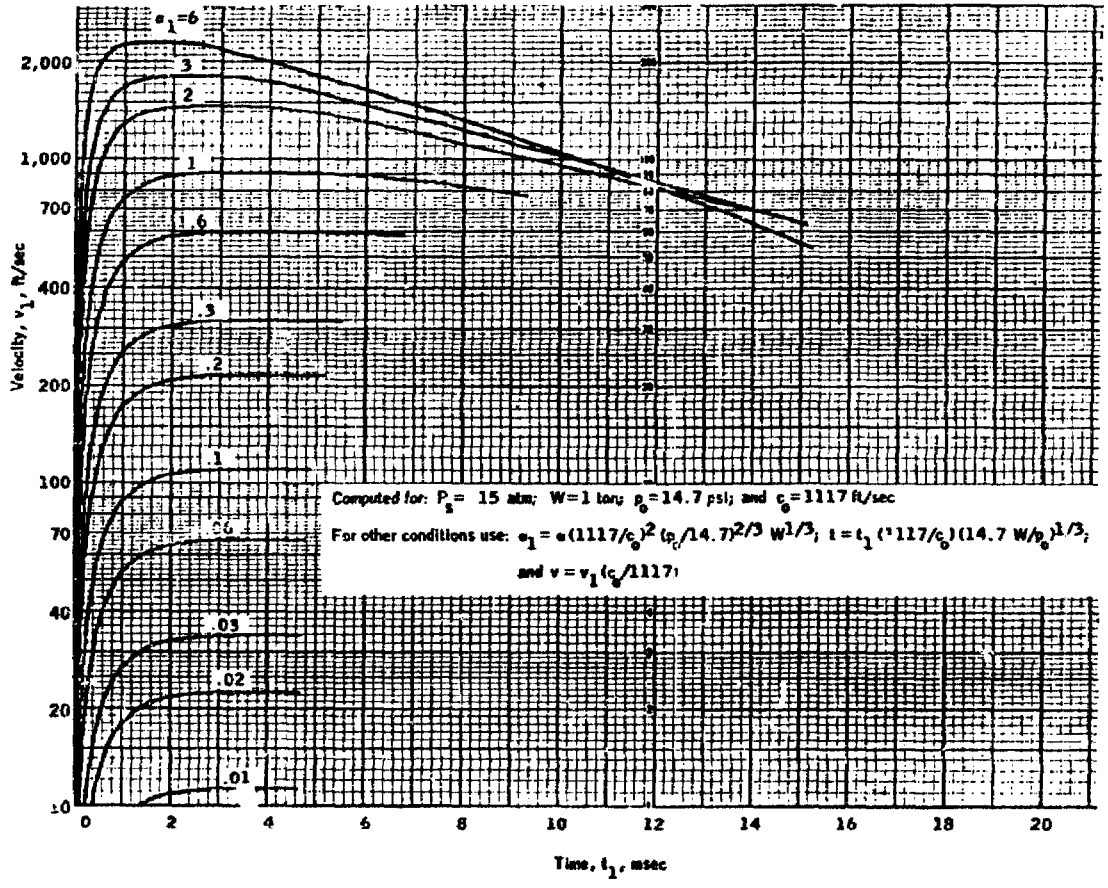


Fig. 3.21 Velocity vs. Time for $P_s$ = 15.0 atm for free-air bursts

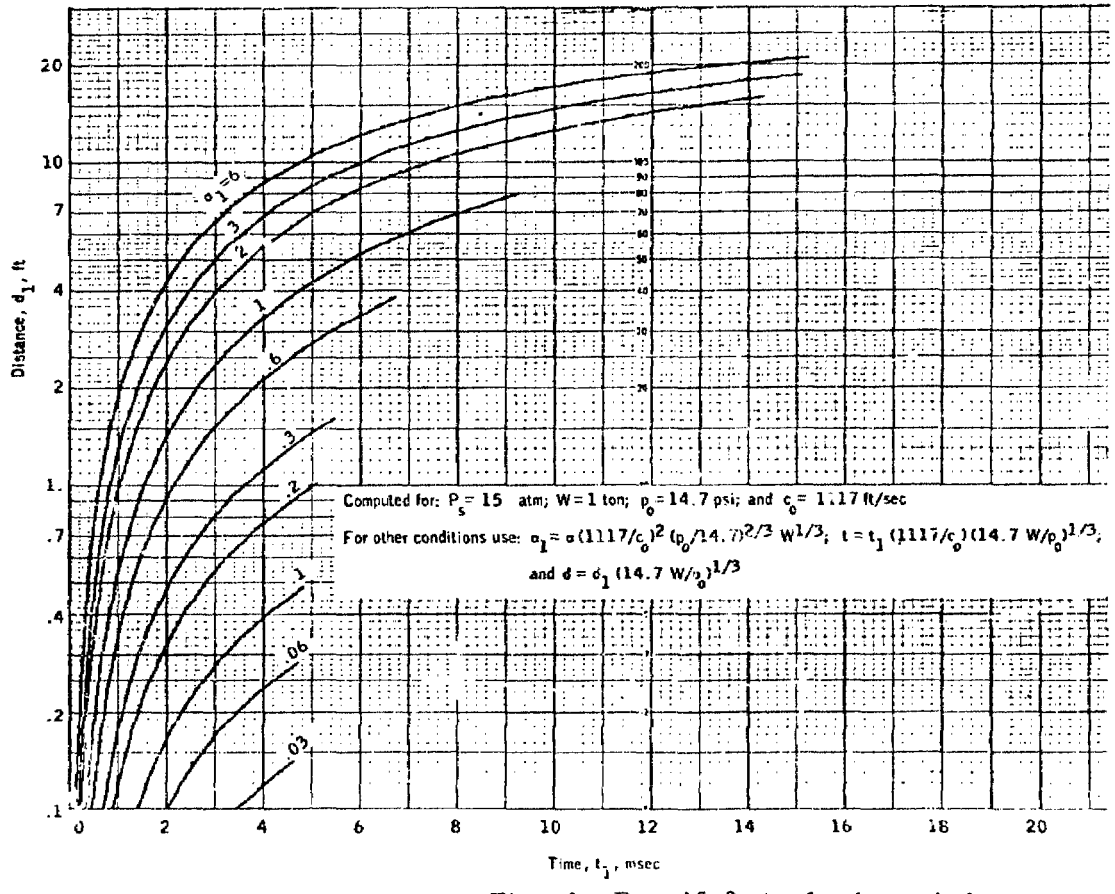


Fig. 3.22 *Distance vs.* Time for $P_s$ = 15.0 atm for free-air bursts

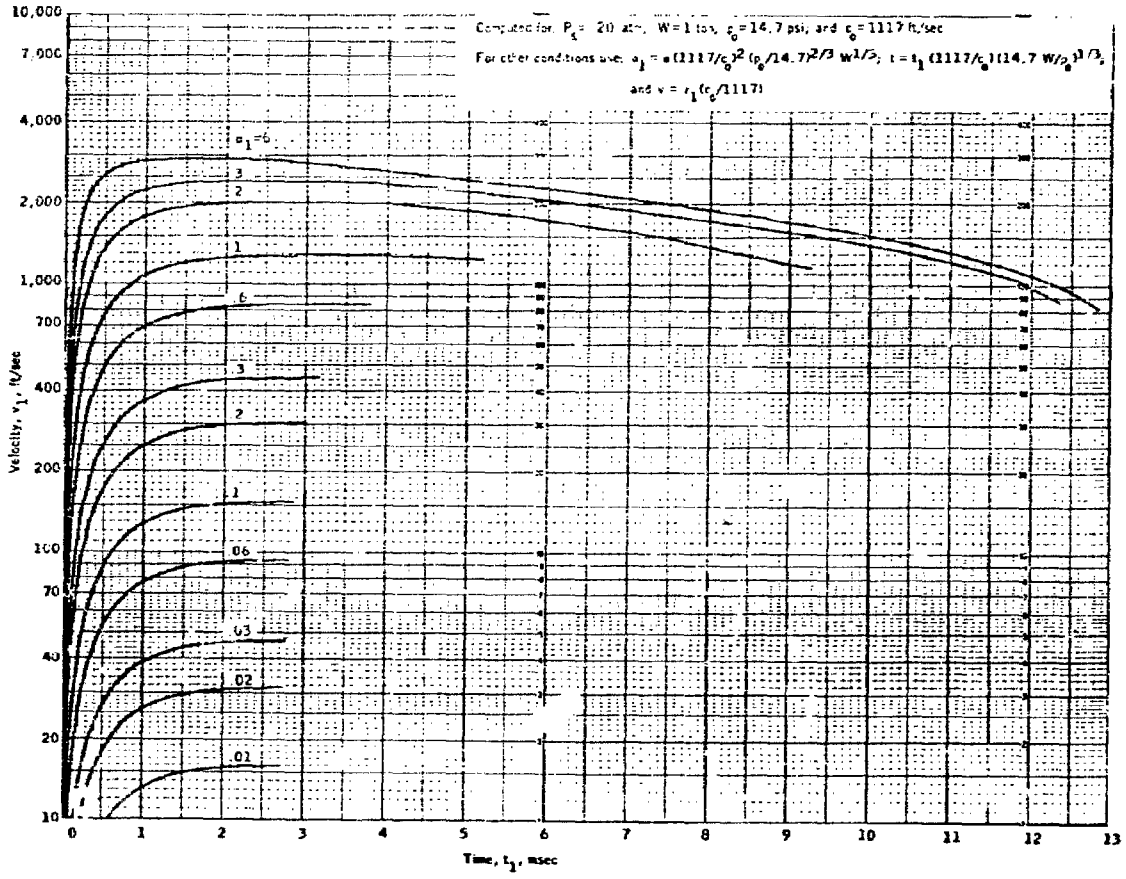


Fig. 3.23 Velocity vs. Time for $P_s$ = 20.0 atm for free-air bursts

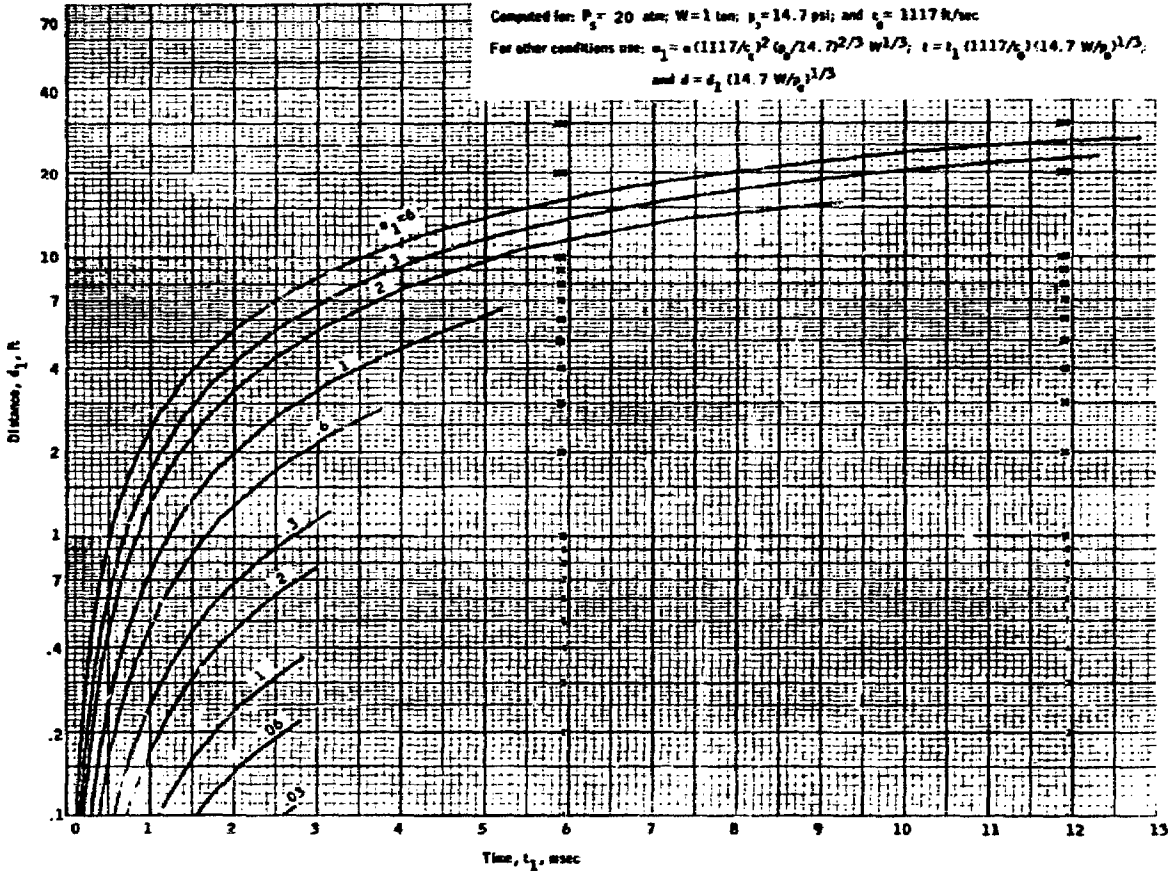


Fig. 3.24 Distance vs. Time for $P_s$ = 20.0 atm for free-air bursts

4.0, 5.0, 6.0, 8.0, 10.0, 15.0, and 20 atms. The velocity curves for $\alpha_1 = 6.0$, in some cases, cross those for the lower acceleration coefficients (see Fig. 3.9, for example). Comparison of the velocity charts with the blast-wave parameters shows that this phenomenon occurs only for blast waves whose dynamic pressure decays relatively fast with time, i.e., blast waves identified with the higher values of "r" listed in Table 2.2.

## 3.3 ACCELERATION VS. TIME

When a blast wave first encounters a missile having zero velocity, the maximum acceleration experienced by the missile is the product of its acceleration coefficient and the maximum dynamic pressure.* Computed values of maximum acceleration in g-units are presented in Table 3.2 for the maximum overpressures and for the acceleration coefficients used in this study. After the missile attains a finite velocity, however, missile and wind velocities also control missile acceleration.* Thus, scaling procedures are not necessary to obtain maximum acceleration, but scaling (as indicated on Figs. 3.25 to 3.36) is necessary to evaluate accelerations occurring after the maximum.

Plots of acceleration vs. time are in Figs. 3.25 to 3.36 for the same combinations of overpressure and acceleration coefficients for which velocity and displacement data were presented in the last section. In order to separate the curves appearing on each chart, the plots were not always made to zero acceleration.

---

*This relation is expressed in Eq. (3) in Chap. 2:

$$a = q\,\alpha\,(u - v)^2/u^2.$$

Table 3.2

Maximum Acceleration (A, g-units) for 12 Acceleration Coefficients ($\alpha$, $ft^2/lb$) and for 12 Maximum Overpressures ($P_s$, atm)

| $P_s$ | $\alpha = 6$ | $\alpha = 3$ | $\alpha = 2$ | $\alpha = 1$ | $\alpha = .6$ | $\alpha = .3$ | $\alpha = .2$ |
|---|---|---|---|---|---|---|---|
| 1.0 | 3,970 | 1,980 | 1,320 | 662 | 397 | 198 | 132 |
| 1.5 | 8,410 | 4,200 | 2,800 | 1,400 | 841 | 420 | 280 |
| 2.0 | 14,100 | 7,060 | 4,700 | 2,350 | 1,410 | 706 | 470 |
| 2.5 | 20,900 | 10,400 | 6,960 | 3,480 | 2,090 | 1,040 | 696 |
| 3.0 | 28,600 | 14,300 | 9,530 | 4,760 | 2,860 | 1,430 | 953 |
| 4.0 | 46,200 | 23,100 | 15,400 | 7,700 | 4,620 | 2,310 | 1,540 |
| 5.0 | 66,100 | 33,100 | 22,000 | 11,000 | 6,610 | 3,310 | 2,200 |
| 6.0 | 87,900 | 44,000 | 29,300 | 14,700 | 8,790 | 4,400 | 2,930 |
| 8.0 | 135,000 | 67,700 | 45,200 | 22,600 | 13,500 | 6,770 | 4,520 |
| 10.0 | 187,000 | 93,400 | 62,300 | 31,100 | 18,700 | 9,340 | 6,230 |
| 15.0 | 325,000 | 162,000 | 108,000 | 54,100 | 32,500 | 16,200 | 10,800 |
| 20.0 | 452,000 | 226,000 | 151,000 | 75,300 | 45,200 | 22,600 | 15,100 |

| $P_s$ | $\alpha = .1$ | $\alpha = .06$ | $\alpha = .03$ | $\alpha = .02$ | $\alpha = .01$ |
|---|---|---|---|---|---|
| 1.0 | 66.2 | 39.7 | 19.8 | 13.2 | 6.62 |
| 1.5 | 140 | 84.1 | 42.0 | 28.0 | 14.0 |
| 2.0 | 235 | 141 | 70.6 | 47.0 | 23.5 |
| 2.5 | 348 | 209 | 104 | 69.6 | 34.8 |
| 3.0 | 476 | 286 | 143 | 95.3 | 47.6 |
| 4.0 | 770 | 462 | 231 | 154 | 77.0 |
| 5.0 | 1,100 | 661 | 331 | 220 | 110 |
| 6.0 | 1,470 | 879 | 440 | 293 | 147 |
| 8.0 | 2,260 | 1,350 | 677 | 452 | 276 |
| 10.0 | 3,110 | 1,870 | 934 | 623 | 311 |
| 15.0 | 5,410 | 3,250 | 1,620 | 1,080 | 541 |
| 20.0 | 7,530 | 4,520 | 2,260 | 1,510 | 753 |

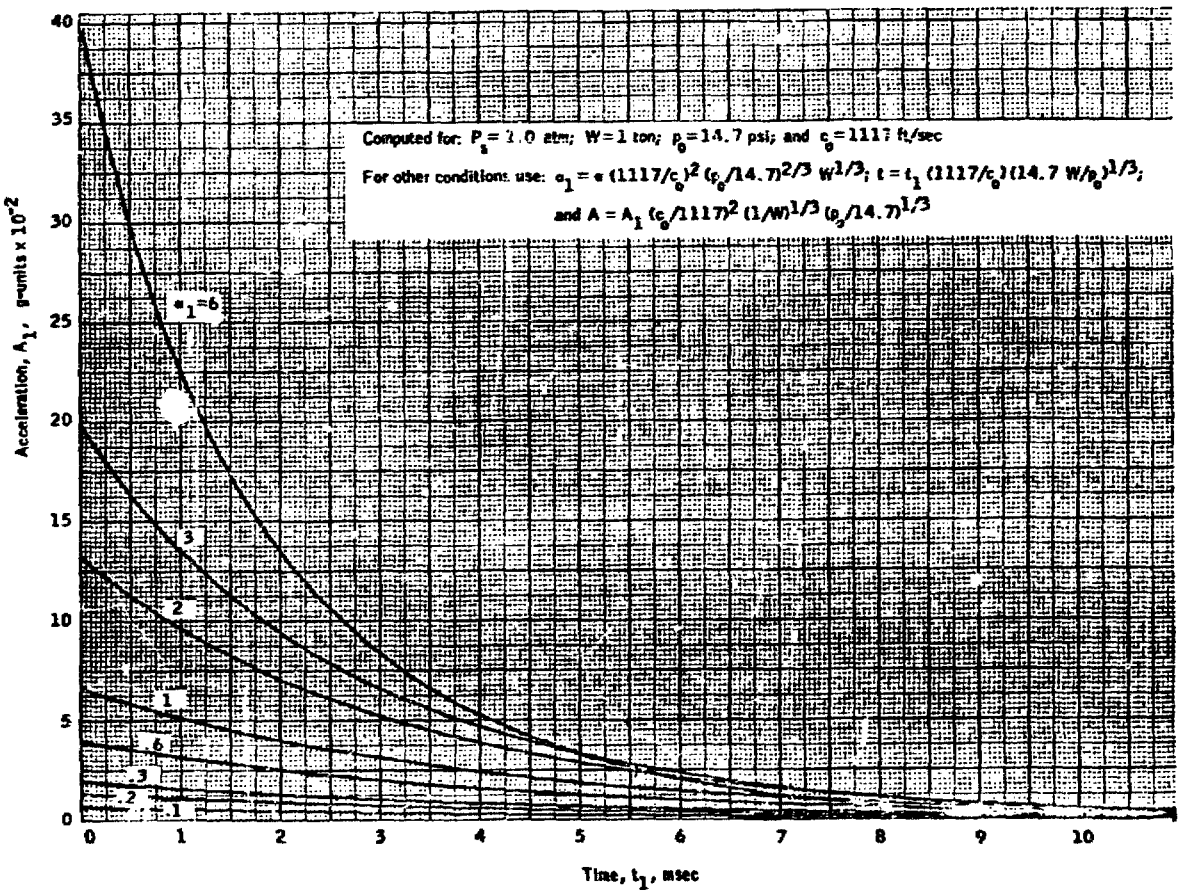


Fig. 3.25 Acceleration vs. Time for $P_s$ = 1.0 atm

W = 1 ton for free-air bursts and 0.5 ton for surface bursts

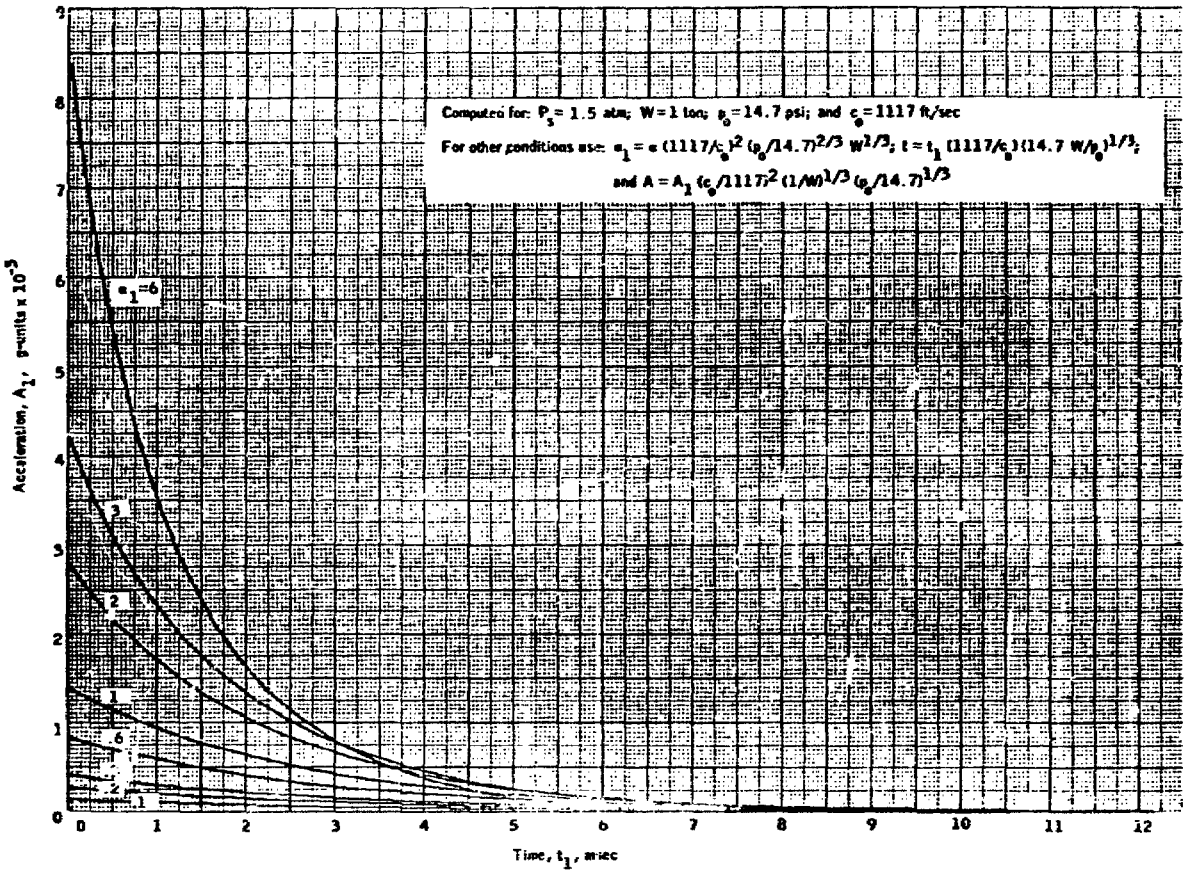


Fig. 3.26 Acceleration vs. Time for $P_s$ = 1.5 atm for free-air bursts

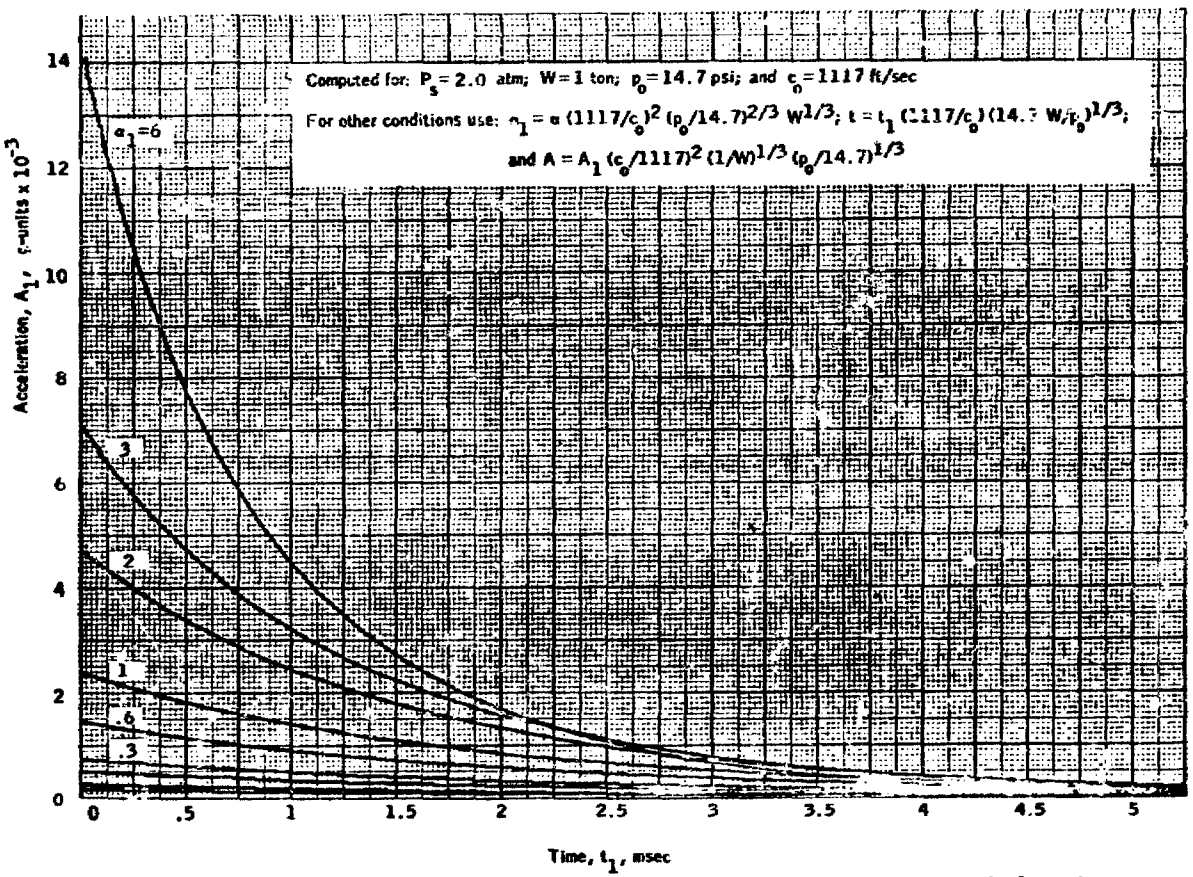


Fig. 3.27 Acceleration vs. Time for $P_s$ = 2.0 atm for free-air bursts

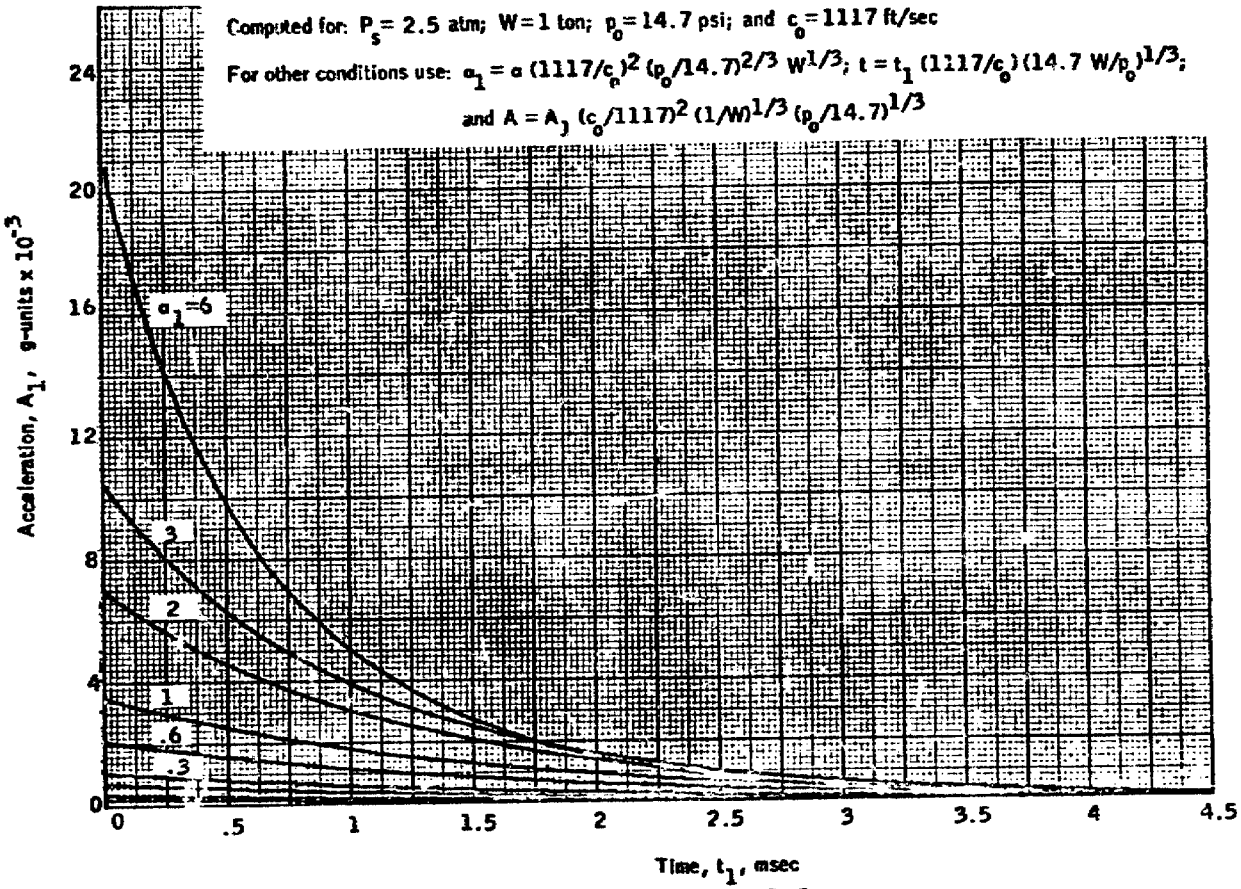


Fig. 3.28 Acceleration vs. Time for $P_s$ = 2.5 atm for free-air bursts

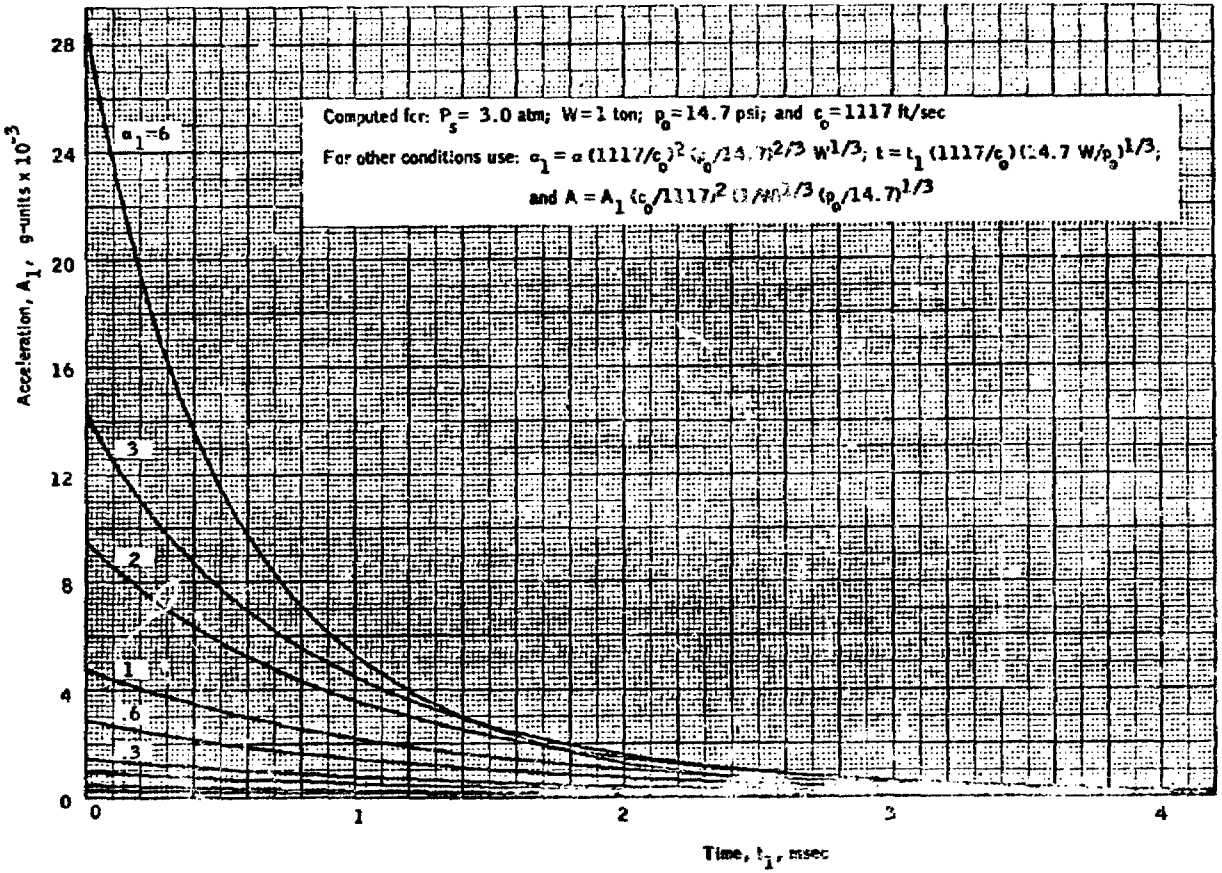


Fig. 3.29 Acceleration vs. Time for $P_s$ = 3.0 atm for free-air bursts

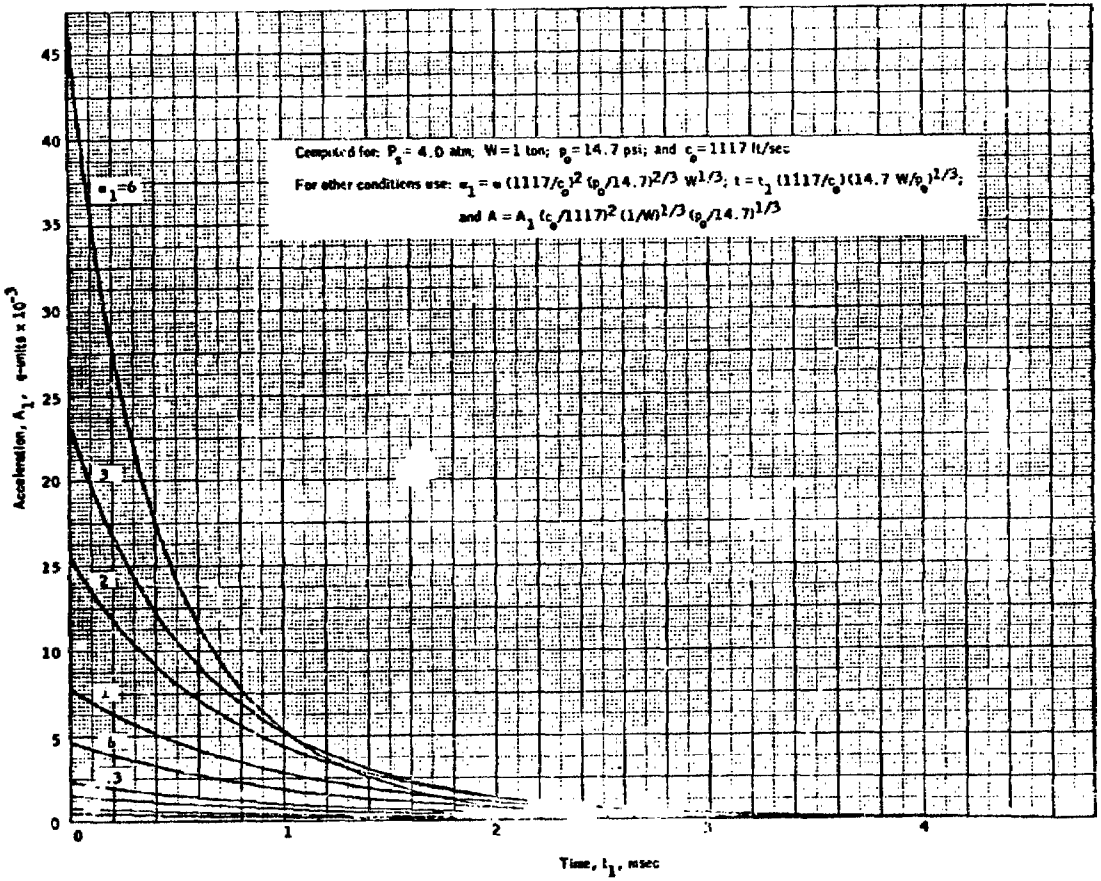


Fig. 3.30 Acceleration vs. Time for $P_s$ = 4.0 atm for free-air bursts

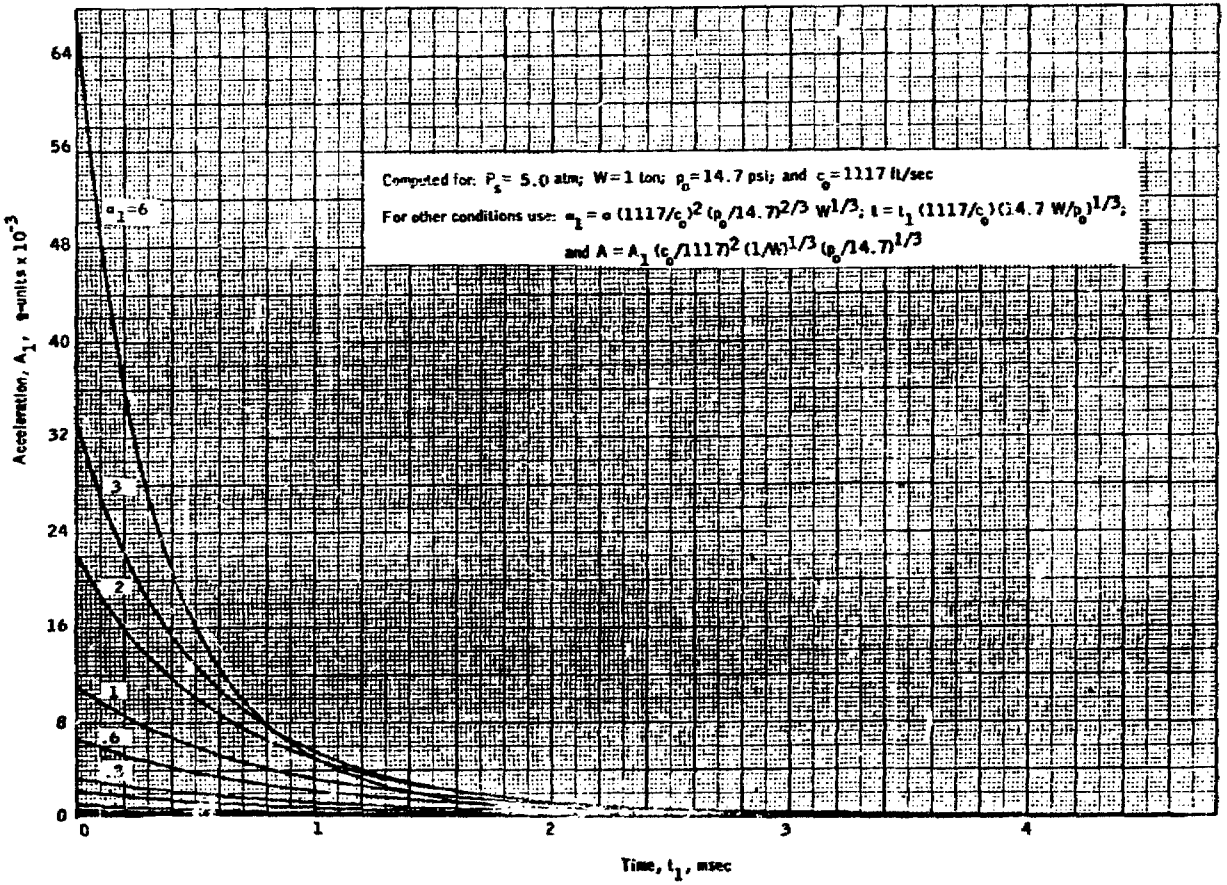


Fig. 3.31 Acceleration vs. Time for $P_s$ = 5.0 atm for free-air bursts

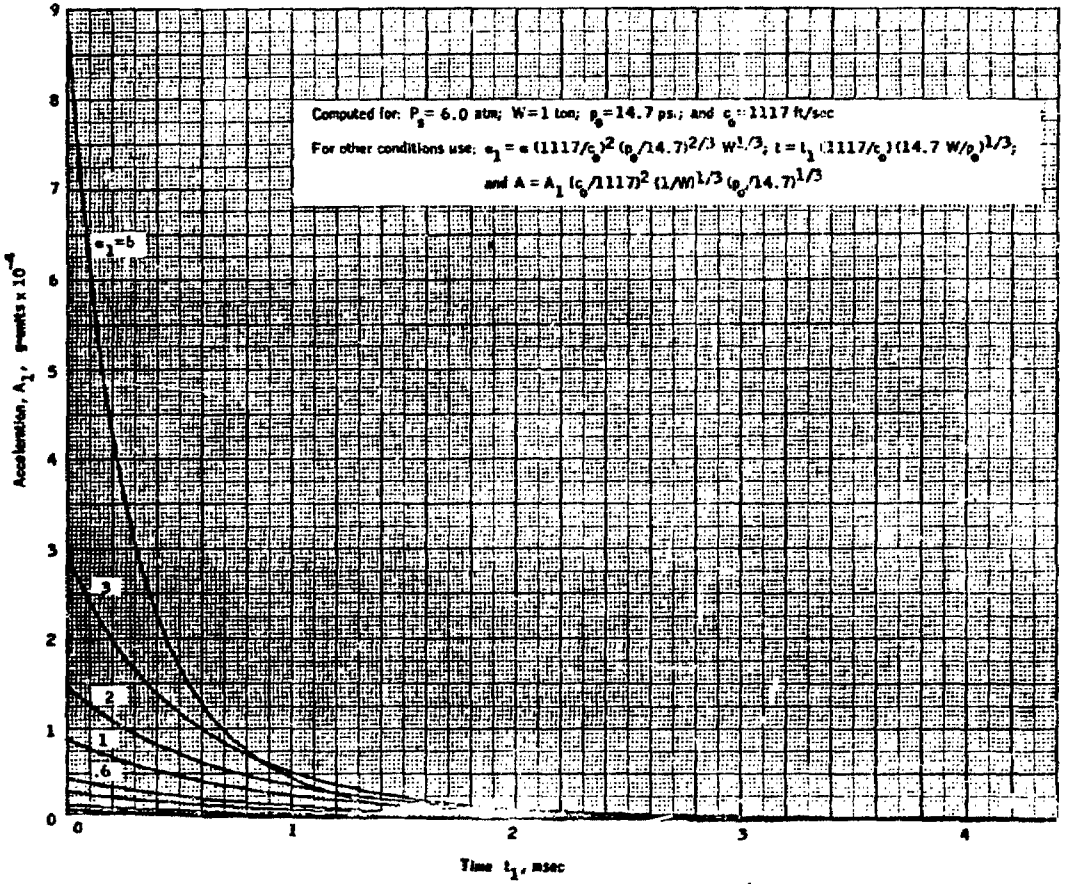


Fig. 3.32 Acceleration vs. Time for $P_s$ = 6.0 atm for free-air bursts

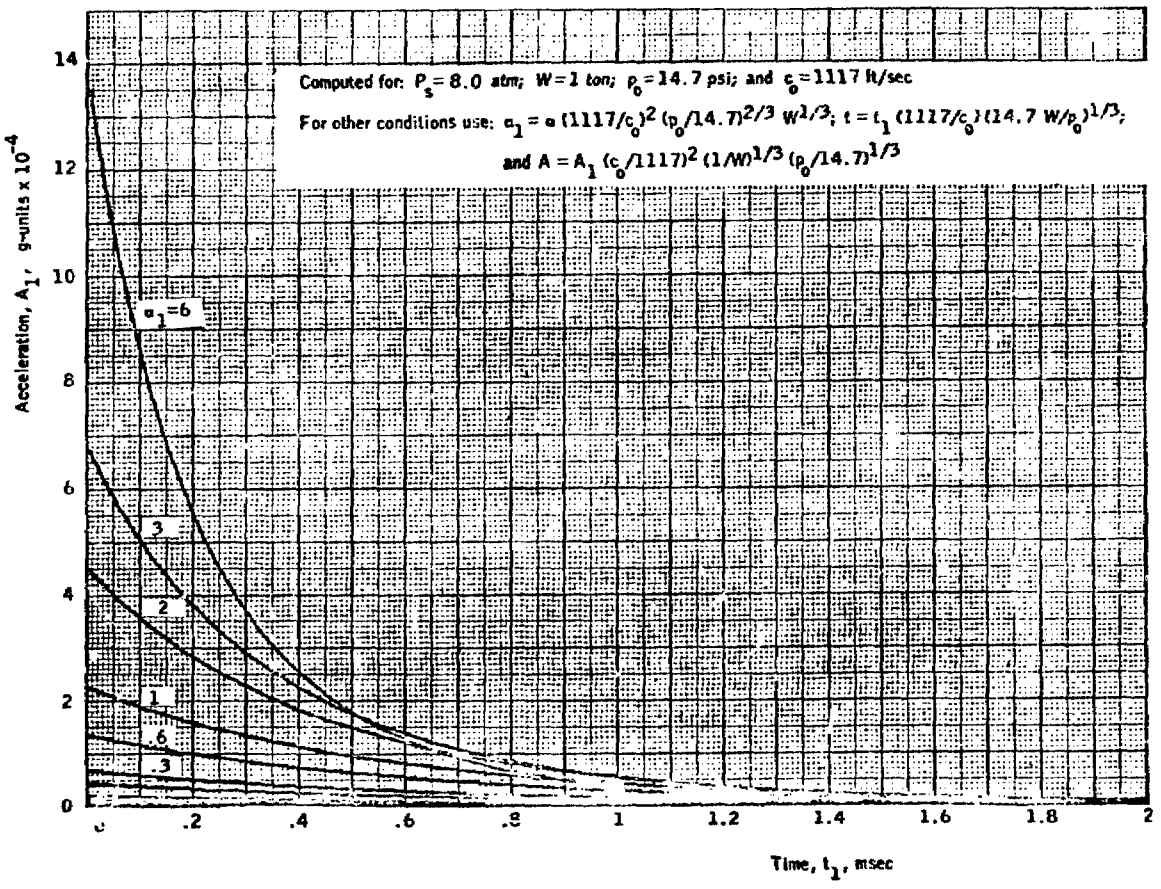


Fig. 3.33 Acceleration vs. Time for $P_s$ = 8.0 atm for free-air bursts

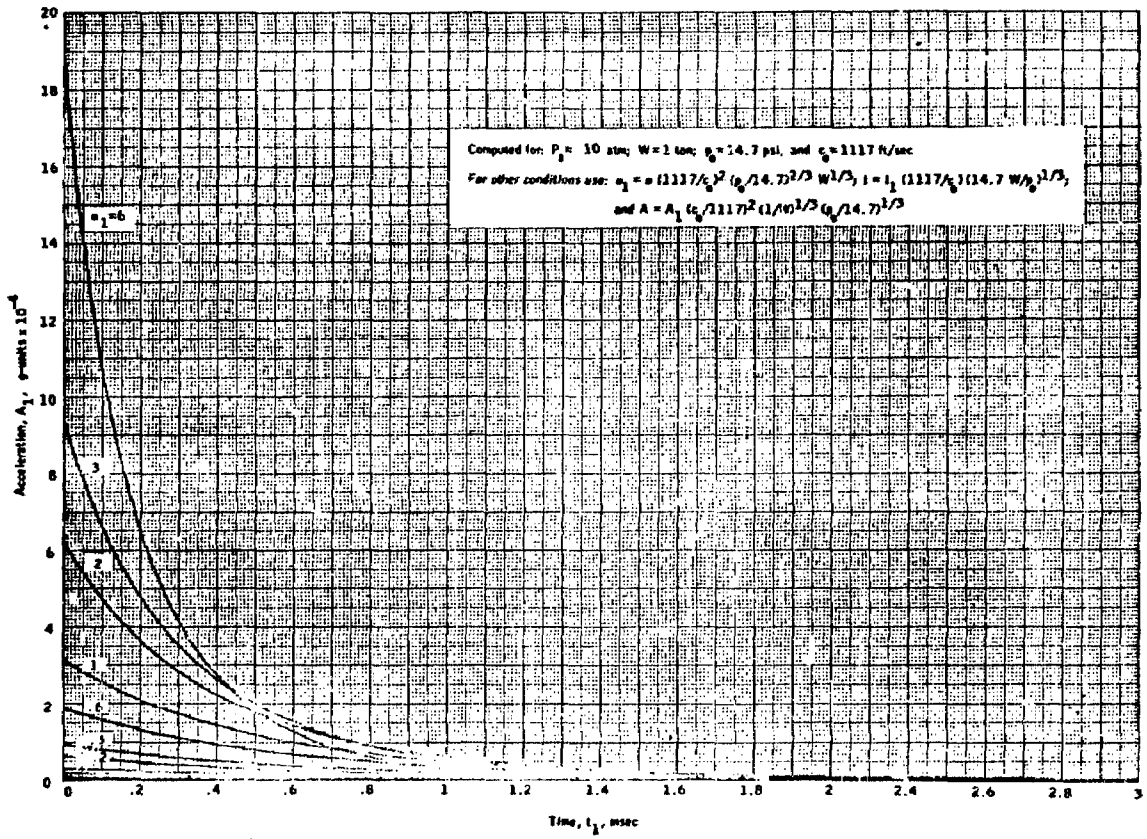


Fig. 3.34 Acceleration vs. Time for $P_s$ = 10.0 atm for free-air bursts

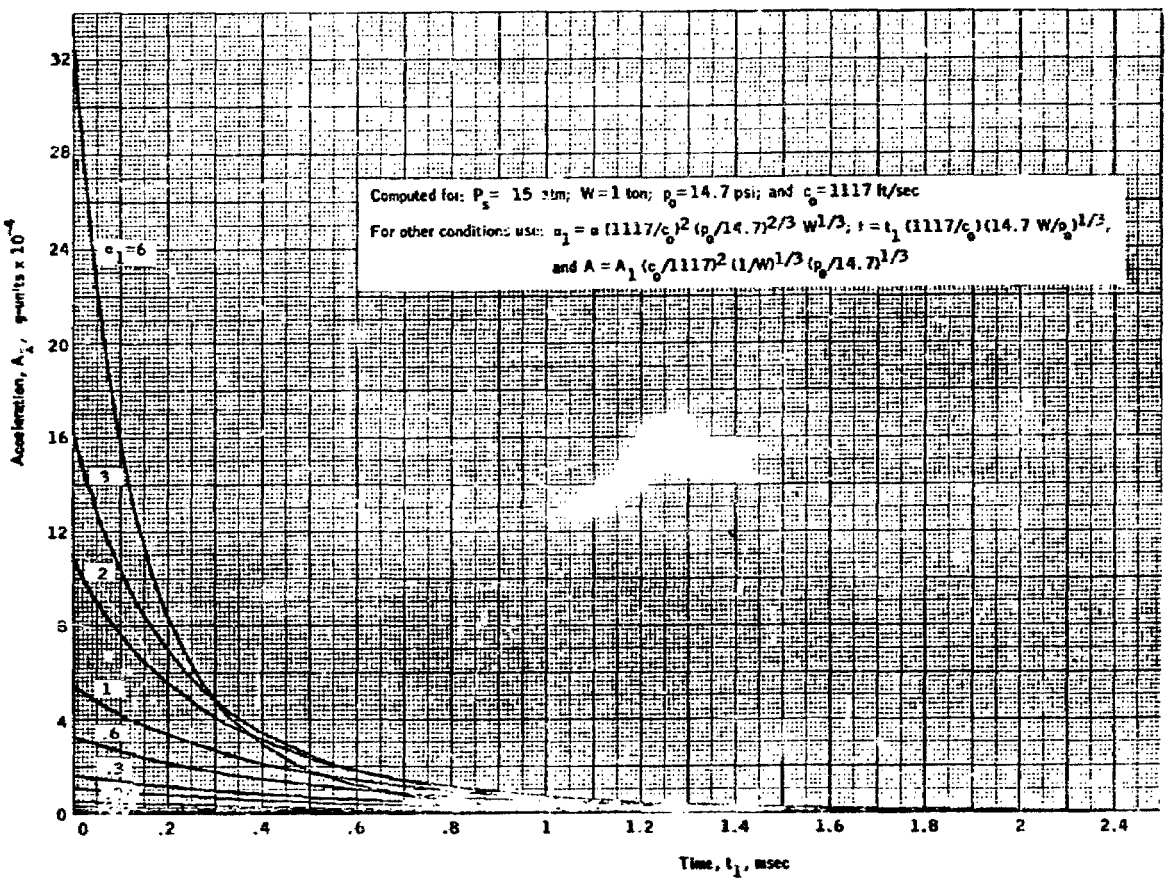


Fig. 3.35 Acceleration vs. Time for $P_s$ = 15.0 atm for free-air bursts

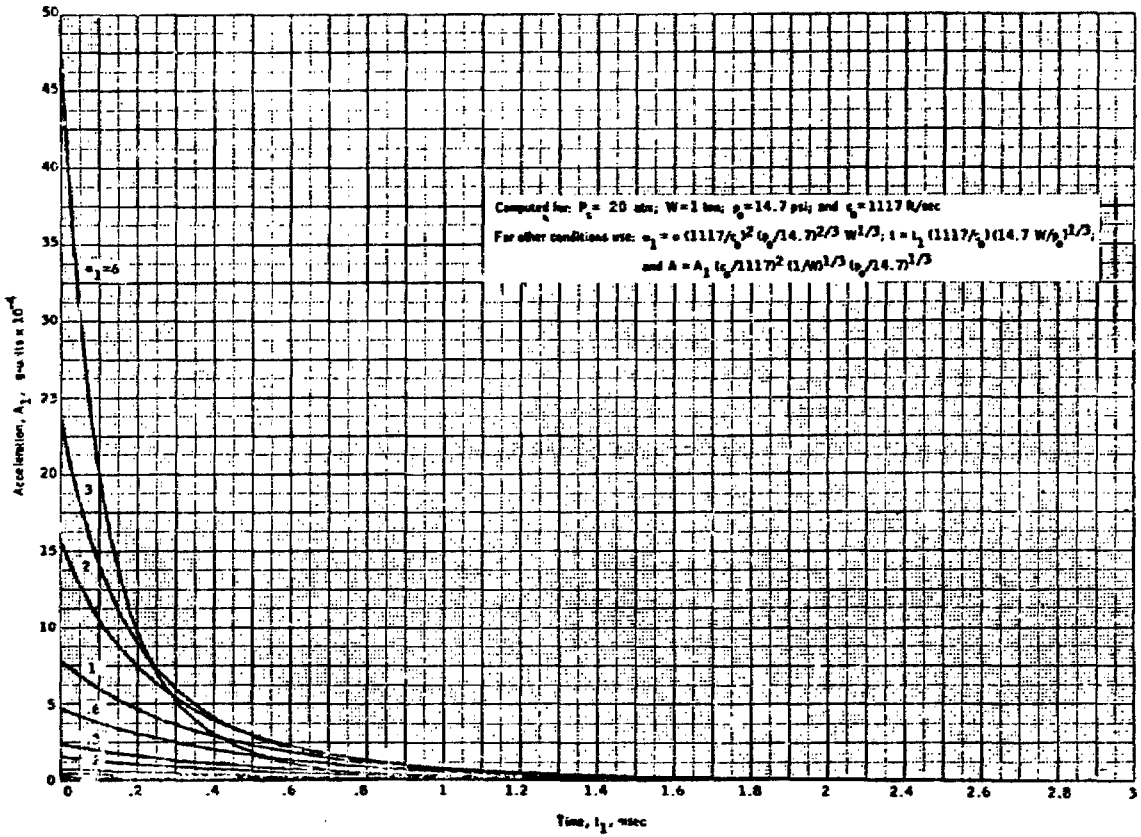


Fig. 3.36 Acceleration vs. Time for $P_s$ = 20.0 atm for free-air bursts

## REFERENCES CHAPTER 3


1. Bowen, I. G., R. W. Albright, E. R. Fletcher and C. S. White, A Model Designed to Predict the Motion of Objects Translated by Classical Blast Waves, Civil Effects Test Operations, USAEC Report CEX-58.9, June 29, 1961.

2. Fletcher, E. R., R. W. Albright, V. C. Goldizen and I. G. Bowen, Determinations of Aerodynamic-Drag Parameters of Small Irregular Objects by Means of Drop Tests, Civil Effects Test Operations, USAEC Report CEX-59.14, October, 1961.

## CHAPTER 4 DISCUSSION

### 4.1 MODEL RELIABILITY

This report presents numerical predictions of the behavior of objects set in motion by high-explosive blast waves. Unfortunately, these predictions cannot be compared with experimental data. The translation model,[1] however, has been successfully used to predict the results of secondary-missile experiments made at the Nevada Test Site with nuclear-produced blast waves which were near ideal (or classical) in character.* In another experiment with anthropomorphic dummies[1,3], maximal velocity could be successfully computed using an average acceleration coefficient for a tumbling dummy. However, to duplicate more precisely the velocity-distance measurements, it was necessary to use an acceleration coefficient which was a function of the orientation of the dummy during translation.

### 4.2 COMPARISON WITH NUCLEAR TRANSLATIONAL EFFECTS

In comparison with results computed for nuclear blast waves, those for high-explosive waves indicate that the overpressure must be considerably higher for an object to attain the same maximum velocity. This velocity occurs, however, after a much shorter distance of translation. Because of the short distances involved, it seems reasonable, in many cases, to assume that a translated man would not change orientation during the accelerative phase of displacement induced by high explosives; thus, a nonvarying acceleration coefficient corresponding to that of his original posture could be used. For example, the charts in Fig. 3.13 and 3.14 for $P_s$ = 5 atm and W = 0.5 ton (surface burst) show that a standing person with an acceleration coefficient of 0.06 $ft^2$/lb would attain a velocity of 23 ft/sec in only 0.1 ft of travel.

A comparison was made in Sect. 3.2 between the velocities predicted using nuclear and high-explosive blast data evaluated for the conditions: $P_s$ = 1 atm, W = 1 kt (surface burst), $p_o$ = 14.7 psi, $c_o$ = 1117 ft/sec.

---

*In these experiments, reported in Ref. 2, the velocities were measured for stones and spheres in open areas and for glass fragments from windows facing the oncoming blast wave. The blast wave entering the houses through the windows was modified; however, if it was assumed to have a maximum overpressure equal to the reflected value of normal incidence, the maximum fragment velocities could be predicted.

For acceleration coefficients of 0.32 and 0.0238 the maximum velocities computed for the two types of burst agreed within 5 per cent. This consistency in the computed results is somewhat surprising in view of the differences in sources of the input blast data. (See Ref. 1, 2, and 3 in Chap. 2.) Nevertheless, field experiments with high explosives similar to those performed with nuclear explosions[2,3] are needed to test the model as well as the input blast data.

## 4.3 BIOMEDICAL INTERESTS

### 4.3.1 General

Those interested in the relation between environmental medicine and weapons effects recognize that any reasonably complete understanding of the many problems involved requires information in the physical, biophysical, and biomedical areas. In this regard, a conceptual guide for analytical procedures and research planning is essential; indeed such has been proposed[4] wherein five problem areas were defined to elucidate the kinds of data needed to establish a quantitative fabric that would allow the source of an environmental variation to be "tied" to hazards assessment.

The five problem areas, plus another concerned with biomedical tasks, are listed in Table 4.1. The first three – encompassing "free-field" scaling, "geometric" scaling and secondary events – represent ground that must be "spaded" mostly by those qualified in the physical sciences if understanding of the environmental variations that can occur at potentially populated locations is to be forthcoming.

Contemplation of the remaining three problem areas make it apparent that hazards assessment requires knowledge of biologic response and the etiologic mechanisms involved. Such knowledge, in turn, touches biomedical tasks such as therapy, rehabilitation and all possible means for minimizing casualties through whatever protective measures might prove effective and feasible. It is here that personnel qualified in biophysics, biology, and medicine can contribute.

### 4.3.2 The Translational Problem

#### Missiles

Since experience has shown that blast-induced environmental variations which are potentially hazardous include the translation of both animate and inanimate objects, applicable and definitive

Table 4.1

**Problem Areas Relevant to Biologic Effects of Nuclear Weapons**

| | | |
|---|---|---|
| Source | Design<br>Yield<br>Burst conditions<br>Range<br>Weather | "Free-field" scaling* |
| Attenuation and Augmentation | Modification of "free-field" phenomena by geometric conditions of exposure | "Geometric" scaling |
| Physical Interaction | Energy transfer to: Physical objects and biological material | Secondary events |
| Biophysical Interaction | Energy dissipation by or within biologic targets | Etiologic mechanisms |
| Biologic Response | Major medical syndromes<br>Isolated individual effects and combined injury | Hazard assessment |
| Biomedical Tasks | Therapeutic and prophylactic measures | Casualty care<br>Rehabilitation<br>Protective procedures |

*See Fig. 4.1 which shows the maximal values of overpressure as a function of range from a 1-ton free-air burst of high explosives at sea level. The chart is useful since it allows one to determine ranges for the overpressures mentioned in Sect. 3.1.

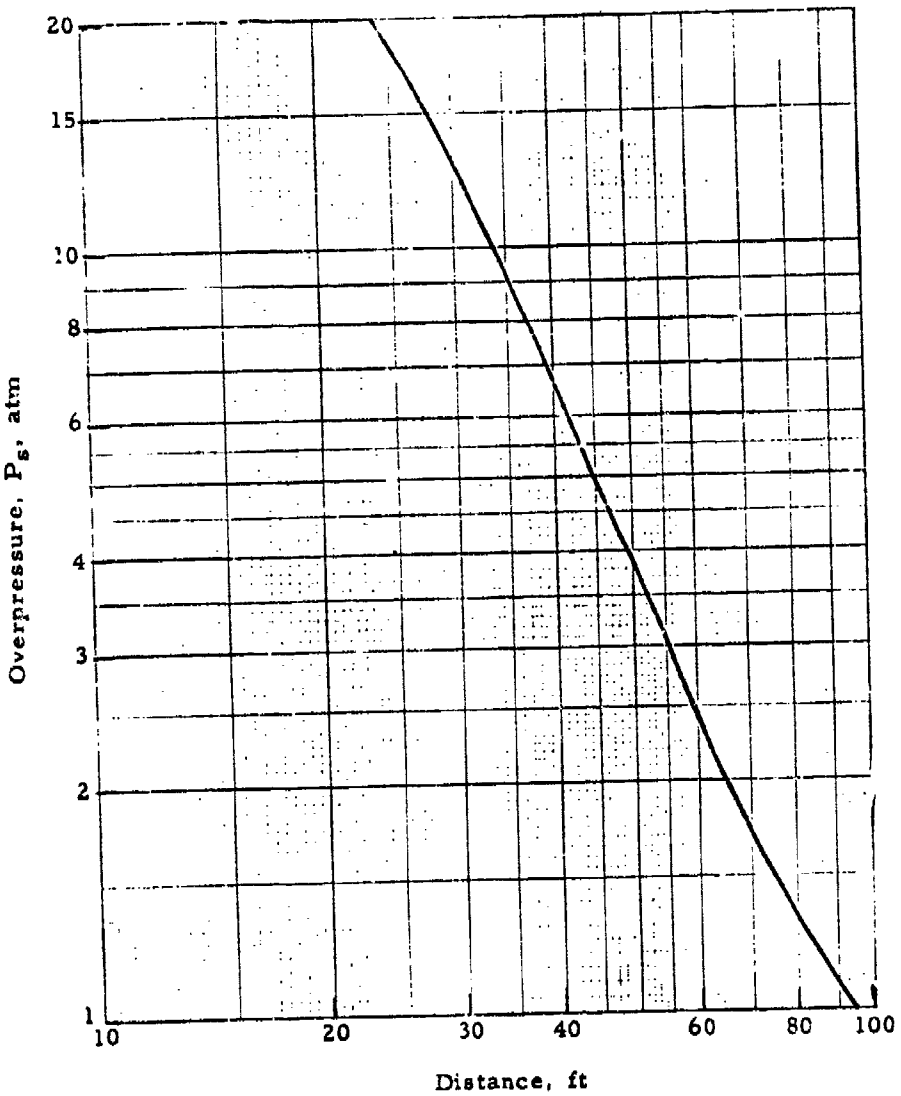


Fig. 4.1. Overpressure vs. distance for free-air burst of 1 ton of high explosives. (Sea-level conditions)

data are required for any comprehensive analysis. For example, among the factors that contribute to the casualty potential of blast-energized missiles are the velocity and angle of impact; the mass density, shape and character of the debris; and the area of the body receiving penetrating and/or nonpenetrating wounds.

Displacement

Similarly, the potential for injury as a consequence of gross displacement of biological targets may be due to accelerative and/or decelerative loading. The former depends at least upon the magnitude of the forces vs. time which initiate displacement and upon the initial and subsequent orientations of the biologic target. The latter depends mostly upon the velocity at which deceleration occurs, the character of the decelerating surface and the area or areas of the body involved whether impacting with a solid object or tumbling over some near-horizontal surface transpires.

4.3.3 Present Study

The previous paragraphs help to place in context the contribution of the analytical data presented in earlier sections of this report in which physical principles were employed to establish a quantitative relationship between free-field blast parameters and the aerodynamic characteristics of objects that may be displaced by blast winds. Thus, one may determine or estimate many of the important physical factors, and the quantitative values associated therewith, that are pertinent to the assessment of environmental hazards.

For example, it is desirable to know what the velocity of debris may be as a function of yield, range, and distance of travel for inanimate objects having various areas, masses, and drag coefficients. Likewise, it is of value to know the order of magnitude and duration of the "G" loads imposed on animate objects by blast winds associated with different overpressures produced by various explosive yields. Also, under similar circumstances, it is helpful to have values for the velocity of animate objects as a function of time and distance of travel. The latter is often pertinent because the work space of one exposed individual may allow only a few feet of travel and thus limit the impact velocity; for another individual the environment may allow attainment of a higher and perhaps maximal velocity before decelerative events occur.

Thus the graphic data prepared for the present study not only contribute to the physical aspects of blast effects, but also offer

information of value to those interested in blast and shock biology as will be noted briefly below.

### 4.3.4 Biological Interests

There are at least two reasons why quantitative data relevant to blast-induced translation of objects interest biomedical personnel. The first is entirely pragmatic, but requires that enough information about biologic response be available to formulate biologic criteria equal to the challenge of hazards assessment. When such criteria exist, it becomes analytically possible to set forth, as functions of yield and range, "safe" areas and those within which performance may be degraded, casualties may occur, and various levels of lethality can be expected.

The second reason physical data relevant to blast-induced environmental variations intrigue blast biologists is related to the fact that biological-response data are frequently lacking or are inadequate for hazards assessment. Under such circumstances the physical information can be used to plan conceptually and to direct more realistic research programs. A case in point concerns the very high initial G-loads predicted for objects the size and shape of man set forth in Table 3.2 and the G-time patterns contained in Figs. 3.25 to 3.36 applicable to the 168-lb man, viz., acceleration coefficient ($\alpha$) values of .052, .021, and .0063 for individuals standing facing the wind, crouching facing the wind, and prone aligned with the wind, respectively. The physical data strictly refer to the displacement of the center of gravity of rigid objects simulating an "average" man. They specify G-loadings that rise "instantaneously" to very high values and decay differently with time depending upon yield, range, acceleration coefficient, etc. They say nothing about the G-time variations that actually occur on the down-stream side of semi-elastic living object compared with the up-stream side or about the associated loads applied to different internal body organs.

The physical data, however, do pose problems for perceptive biologists. For example, what is the biology of instantaneously applied G-loadings? Can high-density blast winds produce injury only because they suddenly "push" a man too fast, and, if so, under what circumstances? Are the significant effects, if any, limited to small explosive charges and to "isolated" portions of the body such as fingers, feet, extremities, etc.? What is the comparative range-yield relationships between these kinds of G-loads and hazards due to primary (pressure) and secondary (missiles) blast effects?

These questions prompt one to be more mundane and say that while the biophysical and biological considerations are simply not the concern of this presentation, it is clear that the physical data at hand, combined with biological information now available, make many comparative assessments possible. In this context the present and similar studies could well focus the light of attention on important portions of the research frontier and perhaps speed full illumination of significant areas in future years.

## REFERENCES CHAPTER 4


1. Bowen, I. G., R. W. Albright, E. R. Fletcher and C. S. White, A Model Designed to Predict the Motion of Objects Translated by Classical Blast Waves, Civil Effects Test Operations, USAEC Report CEX-58.9, June 29, 1961.

2. Bowen, I. G., Mary E. Franklin, E. R. Fletcher and R. W. Albright, Secondary Missiles Generated by Nuclear-Produced Blast Waves, Operation Plumbbob Project 33.2 Report WT-1468 submitted to Mr. L. Joe Deal, Division of Biology and Medicine, U. S. Atomic Energy Commission, on March 7, 1962. (in press)

3. Taborelli, R. V., I. G. Bowen and E. R. Fletcher, Tertiary Effects of Blast – Displacement, Operation Plumbbob Report, WT-1469, May 22, 1959.

4. White, C. S., Biological Effects of Blast, presented before the Armed Forces Medical Symposium, Field Command, Defense Atomic Support Agency, Sandia Base, Albuquerque, New Mexico, November 28, 1961. Submitted as a Technical Progress Report on Contract DA-49-146-XZ-055 to the Defense Atomic Support Agency in December, 1961. Also published as DASA 1271, Defense Atomic Support Agency of the Department of Defense, Washington 25, D. C.

DISTRIBUTION

ARMY AGENCIES

| | |
|---|---|
| Dep Chief of Staff for Mil Ops., DA, Washington 25, DC<br>Attn: Dir of SW&R | 1 |
| Chief of Research & Develop, DA, Washington 25, DC<br>Attn: Atomic Division | 1 |
| Assistant Chief of Staff, Intelligence, DA, Washington 25, DC | 1 |
| Chief Chemical Officer<br>DA, Washington 25, DC | 2 |
| Chief of Engineers<br>DA, Washington 25, DC<br>ATTN: ENGNB | 1 |
| Chief of Engineers<br>DA, Washington 25, DC<br>Attn: ENGEB | 1 |
| Chief of Engineers<br>DA, Washington 25, DC<br>Attn: ENGTB | 1 |
| Chief of Ordnance, DA, Washington 25, DC<br>Attn: ORDTN | 2 |
| Chief Signal Officer, DA, Comb Dev & Ops Div<br>Washington 25, DC<br>Attn: SIGCO-4 | 1 |
| Chief of Transportation, DA, Office of Planning & Intel.<br>Washington 25, DC | 1 |
| The Surgeon General, DA, Washington 25, DC<br>Attn: MEDNE | 2 |
| Commander-in-Chief, U.S. Army Europe,<br>APO 403, New York, N.Y.<br>Attn: OPOT Div, Weapons Branch | 1 |

| | |
|---|---|
| Commanding General<br>U.S. Continental Army Command<br>Ft. Monroe, Va. | 3 |
| Director of Special Weapons<br>Development Office, HQ CONARC,<br>Ft. Bliss, Texas<br>Attn: Capt Chester I. Peterson | 1 |
| President<br>U.S. Army Artillery Board<br>Ft. Sill, Okla | 1 |
| President<br>U.S. Army Aviation Board<br>Ft. Rucker, Alabama<br>Attn: ATBG-DG | 1 |
| Commandant<br>U.S. Army C&GS College<br>Ft. Leavenworth, Kansas<br>Attn: Archives | 1 |
| Commandant<br>U.S. Army Air Defense School<br>Ft. Bliss, Texas<br>Attn: Command & Staff Dept | 1 |
| Commandant<br>U.S. Army Armored School<br>Ft. Knox, Kentucky | 1 |
| Commandant<br>U.S. Army Arty & Missile Sch<br>Ft. Sill, Oklahoma<br>Attn: Combat Dev Dept | 1 |
| Commandant<br>U.S. Army Infantry School<br>Ft. Benning, Ga.<br>Attn: C.D.S. | 1 |
| Commandant<br>Quartermaster School, US Army<br>Ft. Lee, Va.<br>Attn: Ch, QM Library | 1 |
| Commanding General<br>Chemical Corps Training Comd<br>Ft. McClellan, Ala. | 1 |

Commandant
US Army Chemical Corps CBR
Weapons School
Dugway Proving Ground
Dugway, Utah 1

Commandant
US Army Signal School
Ft. Monmouth, N. J. 1

Commandant
US Army Transport School
Ft. Eustis, Va.
Attn: Security & Info Off. 1

Commanding General
The Engineer Center
Ft. Belvoir, Va.
Attn: Asst. Cmdt Engr School 1

Commanding General
Army Medical Service School
Brooke Army Medical Center
Ft. Sam Houston, Texas 1

Commanding Officer
9th Hospital Center
APO 180, New York, N.Y.
Attn: CO, US Army Nuclear
Medicine Research Det, Europe 1

Director
Armed Forces Institute of Path.
Walter Reed Army Med. Center
625 16th St. NW
Washington 25, D.C. 1

Commanding Officer
Army Medical Research Lab,
Ft. Knox, Ky 1

Commandant,
Walter Reed Army Inst of Res.
Walter Reed Army Med Center
Washington 25, D.C. 1

Commanding General
QM R&D Comd,
QM R&D Center
Natick, Mass.
Attn: CBR Liaison Officer 2

Commanding General
QM Research & Engr. Comd, USA
Natick, Mass
(For reports from Opn HARDTACK
only) 1

Commanding General
US Army Chemical Corps
Research & Development Comd.
Washington 25, DC 2

Commanding Officer
Chemical Warfare Lab
Army Chemical Center, Md.
Attn: Tech Library 2

Commanding General
Engineer Research & Dev Lab
Ft. Belvoir, Va.
Attn: Ch, Tech Support Branch 1

Director
Waterways Experiment Station
PO Box 631
Vicksburg, Miss.
Attn: Library 1

Commanding General
Aberdeen Proving Ground
Aberdeen Proving Ground, Md.
Attn: Ballistic Research Lab,
Dir, BRL 2

Commander
Army Ballistic Missile Agency
Redstone Arsenal, Alabama
Attn: ORDAB-HT 1

Commanding General
US Army Electronic Proving
Ground
Ft. Huachuca, Arizona
Attn: Tech Library 1

Director
Operations Research Office
Johns Hopkins University
6935 Arlington Road
Bethesda 14, Md. 1

DISTRIBUTION

NAVY AGENCIES

Chief of Naval Operations
D/N, Washington 25, D.C.
ATTN: OPO3EG — 1

Chief of Naval Operation
D/N, Washington 25, D.C.
ATTN: OP-75 — 1

Chief of Naval Operations
D/N, Washington 25, D.C.
ATTN: OP-922G2 — 1

Chief of Naval Operations
D/N, Washington 25, D.C.
ATTN: OP-91 — 1

Chief of Naval Personnel
D/n, Washington 25, D.C. — 1

Chief of Naval Research
D/N, Washington 25, D.C.
ATTN: Code 811 — 2

Chief
Bureau of Medicine & Surgery
D/N, Washington 25, D.C.
ATTN: Special Wpns Def Div — 1

Chief, Bureau of Ships
D/N, Washington 25, D.C.
ATTN: Code 423 — 1

Chief
Bureau of Yards & Docks
D/N, Washington 25, D.C.
ATTN: D-440 — 1

Director
U.S. Naval Research Laboratory
Washington 25, D.C.
ATTN: Mrs. Katherine H. Cass — 1

Commander
U.S. Naval Ordnance L
White Oak, Silver Sp
Maryland — 2

Director
Material Laborator Code 900)
New York Naval Shipy rd
Brooklyn 1, N.Y. — 1

Commanding Officer
U.S. Naval Mine Defense Lab
Panama City, Fla 1

Commanding Officer
U.S. Naval Radiological Defense
Laboratory, San Francisco
California, ATTN: Tech Info Div 4

Commanding Officer & Director
U.S. Naval Civil Engineering
Lab., Port Hueneme, California
ATTN: Code L31 1

Commanding Officer, U.S. Naval
Schools Command, U.S. Naval
Station, Treasure Island,
San Francisco, California 1

Superintendent
U.S. Naval Postgraduate School
Monterey, California 1

Commanding Officer, Nuclear
Weapons Training Center,
Atlantic, U.S. Naval Base,
Norfolk 11, Va., ATTN:
Nuclear Warfare Dept 1

Commanding Officer, Nuclear
Weapons Training Center,
Pacific, Naval Station,
San Diego, California 1

Commanding Officer, U.S. Naval
Damage Control Tng Center,
Naval Base, Philadelphia 12, Pa
ATTN: ABC Defense Course 1

Commanding Officer
U.S. Naval Air Development
Center, Johnsville, Pa
ATTN: NAS, Librarian 1

Commanding Officer, U.S. Naval
Medical Research Institute,
National Naval Medical Center,
Bethesda, Maryland 1

Officer in Charge, U.S. Naval
Supply Research & Development
Facility, Naval Supply Center,
Bayonne, New Jersey 1

Commandant
U.S. Marine Corps
Washington 25, D.C.
ATTN: Code AO3H 1

DISTRIBUTION

AIR FORCE AGENCIES

Air Force Technical Application
Center, Hq USAF,
Washington 25, D.C. 1

Hq USAF, ATTN: Operations
Analysis Office, Vice
Chief of Staff,
Washington 25, D.C. 1

Air Force Intelligence Center
Hq USAF, ACS/1 (AFOIN-3VI)
Washington 25, D.C. 2

Assistant Chief of Staff
Intelligence, HQ USAFE, APO
633, New York, N.Y. ATTN:
Directorate of Air Targets 1

Director of Research &
Development, DCS/D, Hq USAF,
Washington 25, D.C.
ATTN: Guidance & Weapons
Division 1

Commander
Tactical Air Command
Langley AFB, Virginia
ATTN: Doc Security Branch 1

The Surgeon General
Hq USAF, Washington 25, D.C.
ATTN: Bio-Def Pre Med Div 1

Commander
Tactical Air Command
Langley AFB, Virginia
ATTN: Doc Security Branch 1

Commander
Air Defense Command
Ent AFB, Colorado,
ATTN: Assistant for Atomic
Energy, ADLDC-A 1

Commander, HQ Air Research &
Development Command, Andrews
AFB, Washington 25, D.C.
ATTN: RDRWA 1

Commander, Air Force Ballistic
Missile Division Hq ARDC,
Air Force Unit Post Office,
Los Angeles 45, California
ATTN: WDSOT 1

Commander-in-Chief, Pacific
Air Forces, APO 953, San
Francisco, California, ATTN:
PFCIE-MB, Base Recovery 1

Commander, AF Cambridge
Research Center, L.G. Hanscom
Field, Bedford, Massachusetts,
ATTN: CRQST-2 2

Commander, Air Force Special
Weapons Center, Kirtland AFB,
Albuquerque, New Mexico, ATTN:
Tech Info & Intel Div 5

Directory
Air University Library
Maxwell AFB, Alabama 2

Commander
Lowry AFB, Denver, Colorado
Attn: Dept of Sp Wpns Tng 1

Commandant, School of Aviation
Medicine, USAF Aerospace Med-
ical Center (ATC) Brooks AFB
Tex ATTN: Col Gerrit L. Hekhuis 2

Commander
1009th Sp Wpns Squadron
Hq USAF, Washington 25, D.C. 1

Commander
Wright Air Development Center
Wright-Patterson AFB, Ohio
ATTN: WCOSI 2

Director, USAF Project Rand,
VIA:US Air Force Liaison Office
The Rand Corporation, 1700
Main Street, Santa Monica,
California 2

Commander, Air Defense Systems
Integration Division, L.G.
Hanscom Field, Bedford, Mass
ATTN: SIDE-S 1

Commander, Air Technical Intell-
ingence Center, USAF, Wright-
Patterson Air Force Base, Ohio
ATTN: AFCIN-4Bla, Library 1

DISTRIBUTION

OTHER AGENCIES

Director of Defense Research
and Engineering,
Washington 25, D.C.
ATTN: Tech Library 1

Director, Weapons Systems
Evaluation Group, Room IE880
The Pentagon
Washington 25, D.C. 1

U.S. Documents Officer
Office of the United States
National Military Representa-
tive-SHAPE APO 55, NY., N.Y. 1

Chief
Defense Atomic Support Agency
Washington 25, D.C.
ATTN: Document Library
*Reduce to 3 cys for all FWE reports 4*

| | |
|---|---|
| Commander, Field Command<br>DASA, Sandia Base,<br>Albuquerque, New Mexico | 1 |
| Commander, Field Command<br>DASA, Sandia Base<br>Albuquerque, New Mexico<br>ATTN: FCTG | 1 |
| Commander, Field Command<br>DASA, Sandia Base<br>Albuquerque, New Mexico<br>ATTN: FCWT | 2 |
| Administrator, National<br>Aeronautics & Space Administration, 1520 "H" Street N.W.,<br>Washington 25, D.C., ATTN:<br>Mr. R.V. Rhode | 1 |
| Commander-in-Chief<br>Strategic Air Command<br>Offutt AFB, Nebraska<br>ATTN: OAWS | 1 |
| Commandant<br>U.S. Coast Guard<br>1300 E. Street, NW<br>Washington 25, D.C.<br>ATTN: (OIN) | 1 |

SPECIAL DISTRIBUTION

| | |
|---|---|
| U.S. Atomic Energy Commission<br>Washington 25, D.C.<br>ATTN: Chief, Civil Effects Branch<br>Division of Biology and Medicine | 450 |
| Aberdeen Proving Ground, Md.<br>Ballistic Research Laboratories<br>Terminal Ballistics<br>Attn: Mr. Robert O. Clark, Physicist<br>Mr. William J. Taylor, Physicist | 2 |

Airborne Instruments Laboratory
Department of Medicine and Biological Physics
Deer Park, Long Island, New York
Attn: Mr. W. J. Carberry

Air Force Special Weapons Center
Kirtland Air Force Base
Albuquerque, N.M.
Attn: Mr. R. R. Birukoff, Research Engineer 1

Air Research & Development Command Hqs.
Andrews Air Force Base
Washington 25, D.C.
Attn: Brig. Gen. Benjamin Strickland
Deputy Director of Life Sciences 1

AiResearch Manufacturing Company
9851-9951 Sepulveda Blvd.
Los Angeles 25, California
Attn: Mr. Frederick H. Green, Assistant Chief,
Preliminary Design
Dr. James N. Waggoner, Medical Director 2

AeResearch Manufacturing Company
Sky Harbor Airport
402 South 36th Street
Phoenix, Arizona
Attn: Delano Debaryshe
Leighton S. King 2

American Airlines, Inc.
Medical Services Division
La Guardia Airport Station
Flushing 71, N.Y.
Attn: Dr. Kenneth L. Stratton, Medical Director 1

Brooks Air Force Base
United States Air Force Aerospace Medical Center (ATC)
School of Aviation Medicine
Brooks Air Force Base, Texas
Attn: Brig. Gen. Theodore C. Bedwell, Jr., Commandant
Col. Paul A. Campbell, Chief, Space Medicine
Dr. Hubertus Strughold, Advisor for Research & 3
Professor of Space Medicine

The Boeing Company 3
P. O. Box 3707
Seattle 24, Washington
Attn: Dr. Thrift G. Hanks, Director of Health & Safety
Dr. Romney H. Lowry, Manager, Space Medicine Branch

Dr. F. Werner, Jr., Space Medicine Section
P.O. Box 3815

Chance Vought Astronautics 5
P. O. Box 5907
Dallas 22, Texas
Attn: Dr. Charles F. Gell, chief Life Sciences
Dr. Lathan
Mr. Ramon McKinney, Life Sciences Section
Mr. C. O. Miller
Mr. A. I. Sibila, Manager Space Sciences

Chemical Corps Research & Development Command 2
Chemical Research & Development Laboratories
Army Chemical Center, Md.
Attn: Dr. Fred W. Stemler
Dr. R. S. Anderson

Civil Aeromedical Research Insitiute 1
Oklahoma City, Oklahoma
Attn: Director of Research

Convair Division, General Dynamics Corpn. 2
Fort Worth, Texas
Attn: Mr. H. A. Bodely
Mr. Schreiber

Convair - General Dynamics Corporation 8
Mail Zone 1-713
P. O. Box 1950
San Diego 12, California
Attn: Dr. R. C. Armstrong, Chief Physician
Dr. J. C. Clark, Assistant To Vice-President Engineering
Mr. James Dempsey
Dr. L. L. Lowry, Chief Staff Systems Evaluation Group
Mr. M. H. Thiel, Design Specialist

Dr. R. A. Nau (Mail Zone 6-104)

Mr. W. F. Rector, III (Mail Zone 580-40), P.O. Box 1128

Mr. R. C. Sebold, Vice-President Engineering
Convair General Offices

Defense Atomic Suppor Agency 1
Department of Defense
Field Command
Sandia Base, New Mexico
Attn: Col. S. W. Cavender, Surgeon

The Dikewood Corporation 1
4805 Menaul Blvd., N.E.
Albuquerque, New Mexico

Douglas Aircraft Company, Inc. 2
El Segundo Division
El Segundo, California
Attn: Mr. Harvey Glassner
Dr. E. B. Konecci

Federal Aviation Agency 1
Washington 25, D.C.
Attn: Dr. James L. Goddard, Civil Air Surgeon

Goodyear Aircraft Corporation 1
Department 475, Plant H
1210 Massillon Road
Akron 15, Ohio
Attn: Dr. A. J. Cacioppo

Harvard School of Public Health 1
Harvard University
695 Huntington Avenue
Boston 15, Mass.
Attn: Dr. Ross A. McFarland, Associate Professor
of Industrial Hygiene

Mr. Kenneth Kaplan 1
Physicist
Broadview Research Corporation
1811 Trousdale Drive
Burlingame, Calif.

Lockheed Aircraft Company 1
Suite 302, First National Bank Bldg.
Burbank, California
Attn: Dr. Charles Barron

Lockheed Aircraft Corporation 3
Lockheed Missile and Space Division
Space Physics Department (53-23)
Sunnyvale, California
Attn: Dr. W. Kellogg, Scientific Assistant to
Director of Research
Dr. Heinrich Rose

Lockheed Aircraft Corporation
1122 Jagels Road
Palo Alto, California
Attn: Dr. L. Eugene Root, Missile Systems Director

Lovelace Foundation for Medical Education and Research 50
4800 Gibson Blvd., SE
Albuquerque, N.M.
Attn: Dr. Clayton S. White, Director of Research

The Martin Company 1
Denver, Colorado
Attn: Dr. James G. Gaume, Chief, Space Medicine

McDonnel Aircraft Company
Lambert Field
St. Louis, Missouri
Attn: Mr. Henry F. Creel, Chief Airborne Equipment
Systems Engineer
Mr. Bert North

National Aeronautics and Space Administration 1
1520 "H" Street, N.W.
Washington 25, D.C.
Attn: Brig. Gen. Charles H. Roadman, Acting Director,
Life Sciences Program

Naval Medical Research Institute 1
Bethesda, Md.
Attn: Dr. David E. Goldman, MSC, Commander

Department of the Navy 1
Bureau of Medicine & Surgery
Washington 25, D.C.
Attn: Capt. G. J. Duffner, Director, Submarine Medical Division

North American Aviation 4
International Airport
Los Angeles 45, Calif.
Attn: Scott Crossfield
Dr. Toby Freedman, Flight Surgeon
Mr. Fred A. Payne, Manager Space Planning,
Development Planning
Mr. Harrison A. Storms

Office of the Director of Defense Research & Engineering 1
Pentagon
Washington 25, D.C.
Attn: Col. John M. Talbot, Chief, Medical Services Division,
Room 3D1050 Office of Science

The Ohio State University 2
410 West 10th Avenue
Columbus 10, Ohio
Attn: Dr. William F. Ashe, Chairman, Department of
Preventive Medicine
Dean Richard L. Meiling

The RAND Corporation 2
1700 Main Street
Santa Monica, Calif.
Attn: Dr. H. H. Mitchell, Physics Division
Dr. Harold L. Brode

Republic Aviation Corporation 3
Applied Research & Development
Farmingdale, Long Island, N.Y.
Attn: Dr. Alden R. Crawford, Vice-President
Life Sciences Division
Dr. William H. Helvey, Chief, Life Sciences Division
Dr. William J. O'Donnell, Life Sciences Division

Sandia Corporation 5
P. O. Box 5800
Albuquerque, New Mexico
Attn: Dr. C. F. Quate, Director of Research
Dr. S. P. Bliss, Medical Director
Dr. T. B. Cook, Manager, Department 5110
Dr. M. L. Merritt, Manager, Department 5130
Mr. L. J. Vortman, 5112

System Development Corporation 1
Santa Monica, California
Attn: Dr. C. J. Roach

United Aricraft Company 1
Denver, Colorado
Attn: Dr. George J. Kidera, Medical Director

Laboratory of Nuclear Medicine & Radiation Biology 2
School of Medicine
University of California, Los Angeles
900 Veteran Avenue
Los Angeles 24, California
Attn: Dr. G. M. McDonnel, Associate Professor
Dr. Benedict Cassen

University of Illinois 1
Chicago Professional Colleges
840 Wood Street
Chicago 12, Illinois
Attn: Dr. John P. Marbarger, Director, Aeromedical Laboratory

University of Kentucky 1
School of Medicine
Lexington, Kentucky
Attn: Dr. Loren D. Carlson, Professor of Physiology
& Biophysics

University of New Mexico 1
Albuquerque, New Mexico
Attn: Library

U. S. Naval Ordnance Laboratory 2
White Oak, Maryland
Attn: Capt. Richard H. Lee, MSC
Mr. James F. Moulton

U. S. Naval School of Aviation Medicine 1
U. S. Naval Aviation Medical Center
Pensacola, Florida
Attn: Capt. Ashton Graybiel, Director of Research

Dr. Shields Warren 1
Cancer Research Institute
New England Deaconess Hospital
194 Pilgrim Road
Boston 15, Mass.

Wright Air Development Center 2
Aeromedical Laboratory
Wright-Patterson Air Force Base, Ohio
Attn: Commanding Officer
Dr. Henning E. vonGierke, Chief, Bioacoustics Laboratory

Dr. Eugene Zwoyer 1
Director, Shock Tube Laboratory
P. O. Box 188
University Station
Albuquerque, New Mexico

Armed Services Technical Information Agency 20
Arlington Hall Station
Arlington 12, Virginia

Commanding Officer 1
U. S. Naval Weapons Laboratory
Dahlgren, Virginia